European Journal of Medicinal Chemistry 54 (2012) 483–498

Contents lists available at SciVerse ScienceDirect

European Journal of Medicinal Chemistry

journal homepage: http://www.elsevier.com/locate/ejmech

Original article

Doing the methylene shuffle – Further insights into the inhibition of mitotic kinesin Eg5 with *S*-trityl L-cysteine

Murad N. Abualhasan [a,1,2], James A.D. Good [b,1], Kitiyaporn Wittayanarakul [a], Nahoum G. Anthony [a], Giacomo Berretta [a], Oliver Rath [b], Frank Kozielski [b], Oliver B. Sutcliffe [a], Simon P. Mackay [a,*]

[a] *Strathclyde Institute of Pharmacy and Biomedical Sciences, 161 Cathedral Street, University of Strathclyde, Glasgow G4 0RE, Scotland, UK*
[b] *The Beatson Institute for Cancer Research, Garscube Estate, Switchback Road, Glasgow G61 1BD, Scotland, UK*

ARTICLE INFO

Article history:
Received 24 October 2011
Received in revised form
23 May 2012
Accepted 23 May 2012
Available online 7 June 2012

Keywords:
Mitotic kinesins
Eg5
Antimitotic agents
STLC
Molecular dynamics
KSP

ABSTRACT

S-Trityl L-cysteine (STLC) is an inhibitor of the mitotic kinesin Eg5 with potential as an antimitotic chemotherapeutic agent. We previously reported the crystal structure of the ligand–protein complex, and now for the first time, have quantified the interactions using a molecular dynamics based approach. Based on these data, we have explored the SAR of the trityl head group using the methylene shuffle strategy to expand the occupation of one of the hydrophobic pockets. The most potent compounds exhibit strong (<100 nM) inhibition of Eg5 in the basal ATPase assay and inhibit growth in a variety of tumour-derived cell lines.

1. Introduction

The mitotic kinesin Eg5 (Kif11, Kinesin Spindle Protein, kinesin-5 family) represents an important target for the development of novel antimitotic chemotherapy agents. Current microtubule-based antimitotic chemotherapies have proved broadly effective in the treatment of multiple cancers, however limitations arising due to debilitating peripheral toxicity, innate and acquired resistance and the need to improve on clinical efficacy necessitate novel chemotherapy treatments [1]. The primary function of Eg5 is to form the bipolar spindle during early prometaphase [2,3]; failure to separate the duplicated centrosomes leads to mitotic arrest and ultimately triggers apoptotic cell death in certain tumour cell lines [4,5]. A number of small molecule inhibitors of Eg5 have been developed which are currently undergoing clinical studies [6] (**1**–**3**, Fig. 1), with ispinesib **1** in multiple Phase II clinical trials the most studied and one of the furthest advanced [7–10]. In addition to the clinical inhibitors, a number of other scaffolds have been reported to be potent inhibitors of the mitotic kinesin [6], including *S*-trityl L-cysteine (STLC, **4**, Fig. 1). Initially identified in a screen of compounds from the NCI database [11], STLC selectively inhibits Eg5 with a GI_{50} in the region of 1.2 μM [12]. STLC is an allosteric inhibitor of Eg5 which binds to a pocket formed by helix α2, loop L5 and helix α3 approximately 7 Å from the nucleotide site [13,14]. Reported structure–activity relationship (SAR) studies describe analogues with improved GI_{50} values of 200 nM through introduction of a single *para* lipophilic substituent to a phenyl ring of the trityl group (**5a**–**c**, Fig. 1) [12,15–17]. Herein we report for the first time the quantification of the interaction between STLC and Eg5 at the molecular level using MM/PBSA simulations on the previously

Abbreviations: $cLogD_{7.4}$, calculated $LogD_{7.4}$; cLogS, calculated Log S, where S is the solubility in mol/L; DMEM, Dulbecco's Modified Eagle Medium; Et_2O, diethyl ether; EtOAc, ethyl acetate; GI_{50}, the concentration required to achieve 50% growth inhibition; h, hour; HRMS, high-resolution mass spectrometry; KSP, kinesin spindle protein; MD, molecular dynamics; MeOH, methanol; MM/PBSA, Molecular Mechanics/Poisson-Boltzmann Surface Area; Pgp, P-glycoprotein; RESP, restrained electrostatic potential; R.M.S.D, Root mean square deviation; SAR–activity relationship, structure; STLC, *S*-trityl L-cysteine.

* Corresponding author. Tel.: +44 1415482866; fax: +44 1415526443.
E-mail address: simon.mackay@strath.ac.uk (S.P. Mackay).

[1] These authors contributed equally to the work.
[2] Present address: College of Pharmacy, An-Najah National University, Nablus, Palestine.

0223-5234/$ – see front matter © 2012 Elsevier Masson SAS. All rights reserved.
http://dx.doi.org/10.1016/j.ejmech.2012.05.034

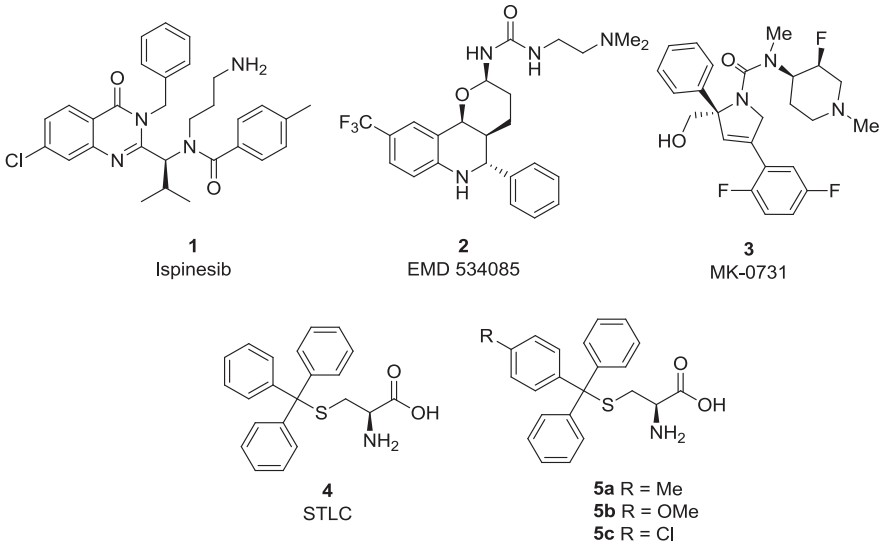

Fig. 1. Eg5 clinical candidates (**1**–**3**), the structure of STLC (**4**) and reported analogues (**5a**–**c**).

determined crystal structure of the complex [13]. Based on these results, we provide further SAR profiling of STLC through chemical modification of the trityl head group.

2. Chemistry

New analogues were prepared by formation of tertiary alcohols before thioetherification with cysteine or cysteamine using boron trifluoride diethyl etherate in acetic acid as described previously (Scheme 1) [12]. Tertiary alcohols **7a**–**l** incorporating a benzyl group were prepared by the reaction of substituted benzophenone analogues with benzylmagnesium chloride (Scheme 1) [18]. Reaction of lithium phenylacetylide with benzophenone at −78 °C afforded alkyne **10** (Scheme 2). Subsequent reduction with Lindlar's catalyst and thioetherification afforded the phenethyl derivative **12**. The benzoyl derivatives **14** and **19** were synthesised by reaction of benzil with phenyllithium followed by thioetherification of the resulting trityl alcohol **13** as described (Scheme 3). For analogues **16a**–**c** with substituents on the benzyl phenyl ring, the intermediate trityl alcohols **15a**–**c** were prepared by *in situ* generation of the Grignard reagent from the appropriately substituted benzyl bromide (Scheme 4) [19,20]. Thioethers incorporating chiral trityl groups were prepared and tested as diastereomeric (**8b**–**8j**) or racemic mixtures (**9b**–**9j**). The ^{13}C NMR spectra of **8b**–**8j** showed that (1*R*,2*R*)- and (1*S*,2*R*)-diastereoisomers had been formed in a 1:1 ratio following the Lewis-acid catalysed alkylation of L-cysteine *via* the planar carbocation intermediate of their respective tertiary alcohols (Supporting Information, Figures S1–S9).

3. Results and discussion

3.1. Decomposition of the binding energies of STLC with Eg5 by MD simulation

The binding free energy of STLC with Eg5 as determined by isothermal calorimetry is −9.6 kcal/mol.[3] The MM/PBSA approach has traditionally produced results consistent with experimental data by sampling structures from an MD trajectory [21]. Calculating the binding free energy of STLC using Eq. (1) through the MM/PBSA approach by extracting energies from MD simulations performed on the components of the complex trajectory returned a binding free energy ($\Delta G_{binding}$) for STLC with Eg5 of −10.6 ± 4.4 kcal/mol; this correlates with the experimentally determined binding free energy.

$$\Delta G_{binding} = \left\langle G_{complex} \right\rangle - \left(\left\langle G_{receptor} \right\rangle + \left\langle G_{ligand} \right\rangle \right) \quad (1)$$

In our study reporting the crystal structure of the Eg5·STLC complex, we provided a qualitative assessment of the interactions in the inhibitor-binding site by investigating those residues in close vicinity (~4 Å) to the inhibitor [13]. To identify the residues of Eg5 that form key interactions with STLC in order to help direct future chemical modification strategies, we decomposed the binding free energy between the inhibitor and individual residues within its binding pocket. This method quantifies ligand-residue enthalpic contributions to the binding free energy by factoring in both short-range van der Waals and long-range electrostatic interactions which may be present (Table 1 and Fig. 2). From these results, we can see that the most significant contribution to the interaction energy is through Glu116 (−12.4 kcal/mol), which forms a hydrogen bond interaction with the amino group. A significant proportion of the amino acids highlighted in Table 1 are charged at physiological pH, thus demonstrating the underlying importance of having a charged ligand to maximise the binding interaction.

We next divided the inhibitor into distinct structural moieties to examine which functionalities of the STLC structure are responsible for these specific inter-residue interactions (Table 2). The hydrophobic phenyl rings of the trityl head group make a significant sum contribution to the ligand's free binding energy of −6.4 kcal/mol. In addition to short range hydrophobic interactions such as S1 with Tyr211 and S3 interacting with the Leu214, long range electrostatic interactions with Glu116, Glu118, Glu128 and Asp130 were also apparent and seem to play a significant part in the free energy of binding of the trityl head. The S2 ring contributes more than either the S1 or S3 rings, demonstrating that the lipophilic interactions of these ring systems could be further optimised. The sulphur atom was shown to have a slight detrimental effect to the binding (0.9 kcal/mol overall). The large stabilizing interaction by the cationic amino group (−10.3 kcal/mol) with the acidic residues Glu116 and Glu118 and the backbone C=O of Gly117 is the most important in terms of the overall contribution to free energy.

[3] Quantification of the binding of STLC and other ligands with Eg5 has been determined by ITC (manuscript in preparation).

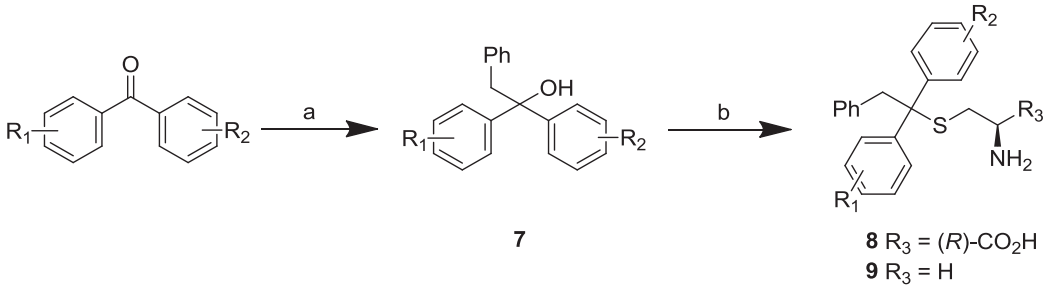

Scheme 1. General route for synthesis of thioethers where R_1/R_2 = H, F, Cl, CH_3 or OH and R_3 = (*R*)-CO_2H or H. Reagents and conditions: (a) $PhCH_2MgCl$, THF, 0 °C to rt, 24 h; (b) L-cysteine (**8**, R_3 = (*R*)-CO_2H) or cysteamine hydrochloride (**9**, R_3 = H), $BF_3{\cdot}Et_2O$, AcOH, 0 °C, 2 h.

Despite the distance between ADP and STLC (~7 Å), there is a long-range electrostatic interaction between the cationic amino group and the anionic diphosphate (−9.1 kcal/mol) of ADP itself, contributing to the inhibitor's ability to prevent the release of the nucleotide from the active site [22,23]. These results support and quantify the SAR studies that have demonstrated the importance of the primary amine group for effective inhibition of Eg5 [12,15]. In contrast, this decomposition method suggests that the carboxylate moiety has a contradictory role. Our crystal structure suggested an attractive interaction between the cationic Arg221 and the carboxylate tail (Fig. 2), which was confirmed (−1.3 kcal/mol), along with the surprisingly more distant Tyr211 (−1.5 kcal/mol). However, overall the interaction appears to be repulsive, particularly with respect to the anionic diphosphate moiety of the nucleotide (+5.7 kcal/mol). This must be compensated for by entropic factors (which are not taken into account by this methodology), since STLC is more potent than its comparable analogue without the carboxylic acid (*vide infra*) [12].

3.2. Structure–activity relationship studies

The presence of acidic residues making electrostatic interactions with the trityl head group suggested that replacement of one phenyl ring with a pyridine could enhance the binding affinity. However, analogues **6** and **18** incorporating a 4-pyridyl moiety (Table 3) displayed lower inhibitory activity in the basal Eg5 ATPase inhibition assay in comparison to the STLC and cysteamine benchmarks **4** and **17**. This suggests that the gains in binding energy obtained through these interactions are more likely from non-polar backbone and methylene groups, rather than the polar side chains. This was more in-line with the binding contributions from Tyr211 with S2 and Leu214 with S3 which suggested lipophilicity as the key feature of binding. The STLC analogue **5a** with a single *para*-methyl modification on the trityl is known to improve on the *in vitro* efficacy of the basic STLC scaffold **4** (Fig. 1) [12]. We therefore rationalized that by performing a methylene shuffle through the introduction of a benzyl moiety, this could afford an improved fit for the S2/S3 phenyl rings buried within the hydrophobic recesses of the binding site. Agreeably, replacing one phenyl with a benzyl afforded a moderate increase in potency over STLC (**8a** *c*/*f* **4**, Table 3). We decided to pursue further SAR investigations based on this modification. Further extensions of the methylene in the linker reduced activity markedly in the case of the phenethyl analogue **12**, whilst functionalisation to a benzoyl abolished inhibition (**14** and **19**, Table 3). For analogues without the carboxylate the potency was generally diminished significantly (e.g. **8a** *c*/*f* **9a**) despite the removal of a potentially repulsive interaction with the bound ADP.

We next investigated whether substituents could be introduced onto the phenyl ring of the benzyl group (**16a**–**c**, Table 3). Introduction of a *meta*-chloro substituent afforded a slight decrease from 138 nM to 240 nM, with the *para*-chloro derivative proving ~3-fold less active. Combining both of these substituents was not favourable, with **16c** only active in the micromolar range. These findings, in conjunction with the weaker activity from phenethyl analogue **12** and lack of inhibition by the ketone analogue **14** indicated that the benzyl occupied a sterically restricted area within the binding site, and that further gains in potency were unlikely to be realised by extending this region of the inhibitor.

We next investigated whether aromatic substituents of other phenyl rings in the benzyl-diphenyl moiety would be tolerated with the aim of optimising the lipophilic interactions of the orthogonal phenyl rings (Table 4). As stated earlier, spectral analysis of the diastereomeric mixtures implied a 1:1 mixture of the (1*R*,2*R*) and (1*S*,2*R*) pairs had been formed. Attempts to separate these using HPLC with either a reverse-phase C18 or a Chiralpak IC chiral column proved unsuccessful. Comparisons therefore between compounds should be viewed from an SAR perspective as relative. Introduction of an *ortho*-fluorine substituent in compound **8b** led to a decrease in IC_{50} activity, demonstrating that while tolerated, this modification was not beneficial overall. However the *meta*-chloro substituent in **8c** was more favourable, and upon switching to a hydrogen-bond donating hydroxy in the *meta* position, a further 2-fold increase in activity was recorded (**8d**, IC_{50} = 67 nM). *Para*-substituted analogues were also well tolerated, with gains in potency achieved relative to the STLC and benzyl-diphenyl benchmarks **4** and **8a**. The presence of a fluoro substituent in the *para* position was tolerated (**8e**, IC_{50} = 150 nM), but the bulkier *para*-chloro substituent improved the basal ATPase IC_{50} to 60 nM for the cysteine analogue **8f**, this mixture proving approximately 2-fold greater than **8a** and 3-fold more potent than STLC **5**. A sterically

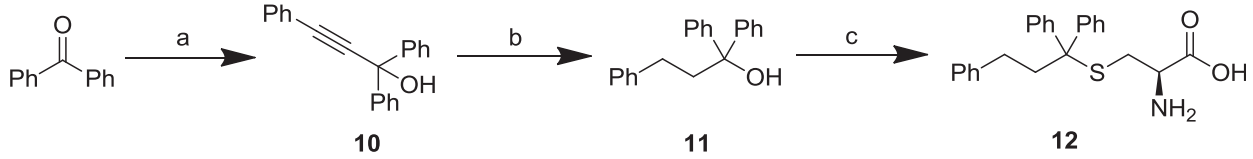

Scheme 2. Reagents and conditions: (a) lithium phenylacetylide, THF, 0 °C, 24 h; (b) H_2, Lindlar's catalyst, K_2CO_3, EtOAc, rt, 72 h; (c) L-cysteine, $BF_3{\cdot}Et_2O$, AcOH, 0 °C, 2 h.

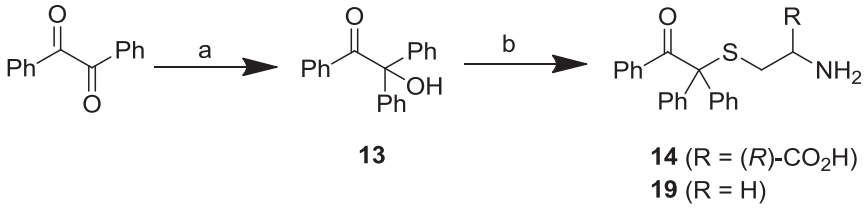

Scheme 3. Reagents and conditions: (a) PhLi, THF, 0 °C to rt, 24 h; (b) L-cysteine (**14**) or cysteamine hydrochloride (**19**), $BF_3 \cdot Et_2O$, AcOH, 0 °C, 2 h.

comparable *para*-methyl analogue **8g** surprisingly was less potent at 168 nM, suggesting the importance of the *para*-chloro substituent was related not only to the sterics but also the electron withdrawing effect on the parent phenyl ring. The electron donating *para*-hydroxy substituent in **8h** was also tolerated with an IC_{50} of 160 nM. Activity was retained in **8i**, which included both *meta*- and *para*-chloro substitutions on a single phenyl ring (IC_{50} = 190 nM), but decreased when compared with either of the singly substituted analogues **8c** or **8f**. In the case of cysteamine analogues without the terminal carboxylate, although introducing substituents to a phenyl ring of the benzyl-trityl moiety also improved the inhibitory activity, in general they proved less potent in the basal ATPase assay than their cysteine analogues (*c*/*f* **8c** and **9c**; **8h** and **9h**). The most potent cysteamine compound was **9f** with a *para*-chloro substituent (IC_{50} = ~140 nM). When analogues with and without the terminal carboxylic acid were compared, the closest in terms of their IC_{50} values were *para*-methyl analogues **8g** and **9g** which were equipotent (IC_{50} = ~170 nM).

Overall, introduction of substituents afforded gains in potency whenever the correct steric (e.g. *meta* or *para*-substituents) and electronic characteristics were satisfied (e.g. electron withdrawing lipophilic substituents or a hydroxyl motif). We next investigated modifications to the third phenyl ring, focussing on fulfilling the hydrophobic interactions which dominate the binding of the trityl group (Table 5). In thioether analogues **8j** and **9j**, incorporating an unsubstituted benzyl ring, a *meta*-chloro phenyl ring and a *para*-chloro phenyl ring, their activities were diminished significantly in comparison to the mono-substituted **8c**, **8f**, **9c**, and **9f**. In this case, the thioethanamine analogue **9j** without the carboxylic acid was more potent than the cysteine analogue **8j**; their poor activity overall however merited no further investigation. Bis-*para*-fluoro substituents were tolerated, but less active than **8e** incorporating a single fluoro substituent in the *para*-position (IC_{50} = ~150 nM). The bis-*para*-chloro analogue **8l** also was less potent than the mono substituted analogue **8f**. Conversely, the bis-*para*-methyl analogue **8m** proved more potent than the comparable mono substituted **8g** (IC_{50} = 106 nM *c*/*f* 167 nM). Aside from the weakly active **9j**, in accord with the prior trend, all cysteine analogues exhibited lower IC_{50} values than their equivalent analogues without the carboxylic acid. This consistently implies that solvent exposure and the concomitant effect on water structure appear to play key roles in this interaction, despite the calculated repulsive influence from ADP (Table 2) [24].

To relate the SAR observed at the ligand level to a structure-based approach with the protein, we examined interactions by docking with GOLD (validated by redocking STLC in the original crystal structure with an RMSD of 0.85 Å [25]). The best ranked pose of each ligand using the Goldscore scoring function was used to visualize its binding mode and evaluate the interactions with Eg5. In the docked pose of the benzyl analogue **8a**, the inhibitor forms the same overall binding interactions as STLC, with the benzyl moiety positioned in the P2 pocket encompassed by Trp127, Asp130 and residues 116–118 (Fig. 3) [13,14]. This forced the sulphur atom closer to the neighbouring Glu116 residue, and pushed the corresponding phenyl ring deeper into the recessed hydrophobic P3 cavity (by approximately 0.96 Å), allowing it to gain enhanced interactions with Leu214 and make contacts with Leu160 at the bottom of the pocket. Our docking studies confirmed that substituents within the benzyl group could not be accommodated (e.g. **12**, **14** and **16a**–**c** *c*/*f* **8a** Table 3). In previous SAR studies on dihydropyrazoles and hexahydro-2*H*-pyrano[3,2-*c*]quinoline based inhibitors, the P2 pocket was found to be sterically constrained and sensitive to substitution (**2** and **3**, Fig. 1) [26,27]. Furthermore, as the phenethyl moiety in **12** is too large to fit in either the P2 or P3 pockets, it is forced in the more polar solvent exposed P1 pocket, which is disfavoured for such a lipophilic group. The crystal structure of Eg5 in complex with a *para*-chloro substituted analogue **5c** has recently been solved by Kaan et al., and demonstrated that the halogen occupied the hydrophobic P3 cavity formed by the Pro137, Leu160, Leu214, Phe239 residues, and the salt bridge between Glu116 and Arg221 [16]. The two-fold increase in activity on incorporation of a *para*-chloro substituent to the benzyl STLC scaffold in **8f** *c*/*f* STLC **4** could therefore be explained by the improved hydrophobic interactions in this pocket. Interestingly, there was no significant difference in the docking scores for the (1*R*, 2*R*) and (1*S*, 2*R*) diastereoisomers, indicating that there is room for interchangeability between the pockets depending on the phenyl substituents. Our docking studies constantly placed the benzyl group in the P2 position, independent of substituent nature or the presence of the carboxylate.

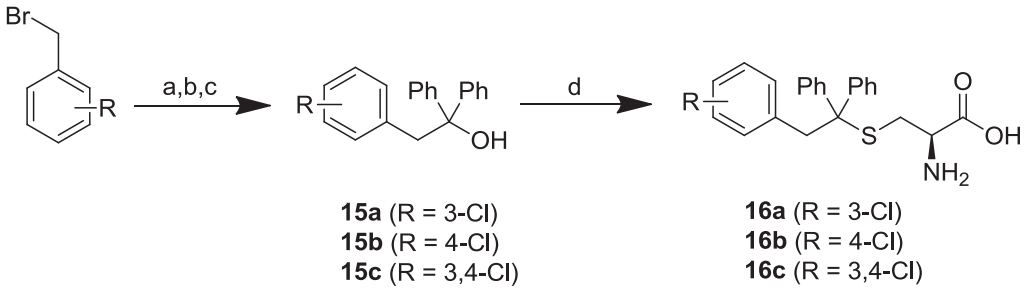

Scheme 4. Reagents and conditions: (a) cat. I_2, Mg, 50 °C, 1 h; (b) Et_2O, rt, 3 h; (c) Ph_2CO, Et_2O, rt, 24 h; (c) L-cysteine, $BF_3 \cdot Et_2O$, AcOH, 0 °C, 2 h.

Table 1
Decomposition of the binding free energies between individual residues of Eg5 with STLC ($\Delta G \leq -1.0$ kcal/mol and $\Delta G \geq 1.0$ kcal/mol).

Residue no.	Binding free energies (kcal/mol)
Arg26	1.7
Lys111	1.9
Glu116	−12.4
Asp130	−2.4
Arg138	1.7
Glu162	−1.9
Asp170	−1.6
Tyr211	−2.0
Leu214	−2.2
Arg221	2.2
Asp265	−2.7

3.3. Evaluation of growth inhibition

We evaluated twelve of the most potent compounds and STLC in growth inhibition assays against the human leukaemia tumour cell line K562, and additionally examined the cytotoxicity of five in colon, lung and pancreatic cell lines (Table 6). In general the activity levels displayed in the basal ATPase assay against the enzyme did not translate to strong inhibition of the selected tumour cell lines. In the human leukaemia K562 cell line the most potent of the benzyl analogues was **8g** with a *para*-methyl, benzyl group and carboxylic acid ($GI_{50} = 1.4$ μM), equipotent with STLC **4**. Surprisingly, **8d** and **8h** with a *meta*- and *para*-hydroxy substituent respectively, proved substantially less active when evaluated in the K562 cell assay, despite strong ATPase inhibition. The *meta*-hydroxy analogue **9d** without the carboxylate was also examined to evaluate whether the poor activity observed in **8d** and **8h** was due to the dual presence of the carboxylic acid and phenolic hydroxyl adversely affecting cell permeability. Analogue **9d** proved approximately 6-fold more active, suggesting this was an important factor. Across the colon, lung and pancreatic cancer derived tumour cell lines **4** proved the most potent. Of the benzyl analogues examined in the colon cell line HCT116, the *para*-methyl derivative **9g** without the carboxylate was most potent ($GI_{50} = \sim 1.2$ μM). In the NCI-H1299 lung cancer cell line **9g** and the equivalent cysteine containing analogue **8g** were the most potent of the new analogues, with GI_{50} levels of ~2.4 μM and 2.5 μM. However in the pancreatic cell line BxPC3, all four analogues examined proved approximately equipotent, in the region of 4 μM. This was the cell line in which the benzyl-substituted analogues were least effective. Overall, the *para*-methyl analogues **8g** and **9g** with and without the carboxylic acid were approximately equipotent, which is reflective of their comparable IC_{50} values, whilst for the *para*-chloro substituted

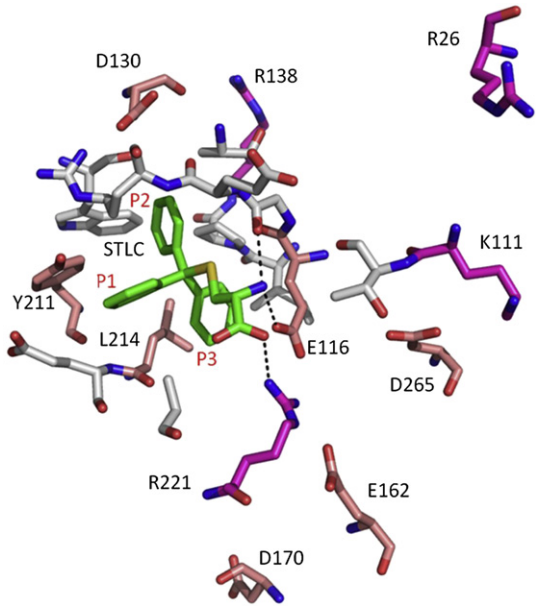

Fig. 2. Crystal structure of STLC with Eg5 (PDB entry 2WOG, chain A), highlighting residues contributing most to the binding free energy. Carbon atoms are displayed in magenta for positive ΔG and pink for negative ΔG contributions, based on Table 2. Hydrogen bonds between the ligand and receptor are marked as dotted lines. (For interpretation of the references to colour in this figure legend, the reader is referred to the web version of this article.)

Table 2
The functional groups (subsites S1–S6) of STLC and the binding free energies (kcal/mol) between residues in Eg5 and each subsite of STLC.

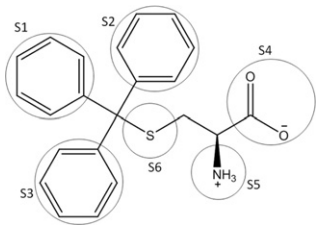

Residue	S1	S2	S3	S4	S5	S6
ADP	–	–	–	5.7	−9.1	–
Mg^{2+}	–	0.7	1.1	–	1.5	2.0
Gln78	–	–	–	–	0.6	–
Gly110	–	–	–	–	0.5	–
Lys111	–	–	–	–	2.2	–
Met115	–	–	–	–	0.9	–
Glu116	–	−1.1	−0.7	1.0	−3.5	–
Gly117	–	0.6	–	–	−3.7	–
Glu118	–	−2.3	–	0.6	−1.0	−0.5
Glu128	–	−0.6	–	–	–	–
Asp130	–	−1.3	–	–	–	–
Ala133	–	1.1	–	–	–	–
Ile136	–	–	–	–	0.7	−0.6
Pro137	–	–	0.8	–	–	–
Tyr211	−1.6	–	–	−1.5	–	–
Leu214	0.6	–	−1.8	–	–	–
Glu215	−0.7	–	−0.7	–	–	–
Arg221	–	–	–	−1.4	0.8	–
Asp265	–	–	−0.5	–	–	–
Total	−1.7	−2.9	−1.8	4.4	−10.3	0.9

Table 3
Effect on basal ATPase activity of Eg5 when one phenyl ring in STLC is replaced.

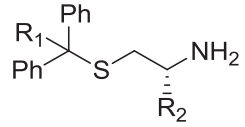

Cmpd	R_1	R_2	Inhibition of basal ATPase activity IC_{50} [nM]
4 (STLC)	Ph	(*R*)-CO_2H	185.9 ± 20.5
6	4-Pyridyl	(*R*)-CO_2H	514.2 ± 66.6
8a	$PhCH_2$	(*R*)-CO_2H	138.0 ± 11.2
9a	$PhCH_2$	H	684.5 ± 81.0
12	$PhCH_2CH_2$	(*R*)-CO_2H	15,836 ± 3817
14	PhCO	(*R*)-CO_2H	>150,000
16a	3-Cl-$PhCH_2$	(*R*)-CO_2H	237.5 ± 11.6
16b	4-Cl-$PhCH_2$	(*R*)-CO_2H	455.8 ± 86.5
16c	3,4-Cl-$PhCH_2$	(*R*)-CO_2H	5278 ± 376
17	Ph	H	241.2 ± 19.8
18	4-Pyridyl	H	942.2 ± 182.4
19	PhCO	H	>50,000

Table 4
Effect on basal ATPase activity of Eg5 when one phenyl ring in STLC is replaced by a benzyl group, and a second phenyl ring modified.

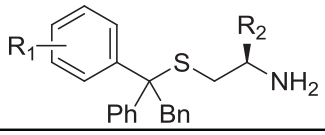

Cmpd	R_1	R_2	Inhibition of basal ATPase activity IC_{50} [nM]
8b	2-F	(*R*)-CO_2H	216.8 ± 19.2
8c	3-Cl	(*R*)-CO_2H	128.9 ± 15.8
8d	3-OH	(*R*)-CO_2H	67.6 ± 7.4
8e	4-F	(*R*)-CO_2H	150.5 ± 10.7
8f	4-Cl	(*R*)-CO_2H	58.6 ± 7.4
8g	4-CH_3	(*R*)-CO_2H	167.6 ± 18.1
8h	4-OH	(*R*)-CO_2H	159.4 ± 15.7
8i	3,4-Cl	(*R*)-CO_2H	191.2 ± 20.1
9b	2-F	H	789.5 ± 42.8
9c	3-Cl	H	519.0 ± 86.4
9d	3-OH	H	256.1 ± 34.6
9e	4-F	H	577.9 ± 23.6
9f	4-Cl	H	140.9 ± 16.2
9g	4-CH_3	H	171.9 ± 15.4
9h	4-OH	H	665.6 ± 179.9
9i	3,4-Cl	H	229.3 ± 21.1

pair **8f** and **9f**, the cysteine analogue was significantly more active in three of four cell lines, and equipotent in the colon cell line.

3.4. Physicochemical profile

One rationale for the reduction in activity observed on translation of the inhibitors from the basal assay into cells is a poorly suitable physicochemical character. *In silico* calculations were performed for the ALogP, $cLogD_{7.4}$, cLogS for all new analogues (data not shown). While incorporation of a benzyl unit did not compromise the LogP and $LogD_{7.4}$ beyond reasonable limits for cell penetration (e.g. cLogD7.4 STLC **4** = 1.73; **8a** = 2.06; **5a** = 2.25; **8g** = 2.55) [28], it did impact on the solubility. The calculated LogS for STLC was −7.07 *vs* −7.49 for **9a** and −7.60 for STLC analogue **5a** *vs* −8.02 for comparable benzyl analogue **9g** with a *para*-methyl substituent. We therefore determined the turbidimetric solubility for STLC and benzyl analogues **8a**, **8g**, **9a** and **9g** at pH = 7.4. While STLC, **8a** and **9a** all proved soluble (>100 μM), **8g** and **9g** were poorly soluble with solubilities of 11.5 μM and 6.5 μM respectively. This therefore provides one explanation for the reduction in the levels of cellular growth inhibition recorded, despite the improvement on the basal inhibition levels upon introduction of a lipophilic substituent.

Table 5
Effect on basal ATPase activity of Eg5 when one phenyl ring in STLC is replaced by a benzyl group, and both remaining phenyl rings are modified.

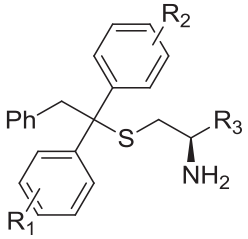

Cmpd	R_1	R_2	R_3	Inhibition of basal ATPase activity IC_{50} [nM]
8j	3-Cl	4-Cl	(*R*)-CO_2H	567.5 ± 56.9
8k	4-F	4-F	(*R*)-CO_2H	178.2 ± 19.6
8l	4-Cl	4-Cl	(*R*)-CO_2H	251.8 ± 29.2
8m	4-CH_3	4-CH_3	(*R*)-CO_2H	106.5 ± 16.1
9j	3-Cl	4-Cl	H	436.7 ± 36.0
9k	4-F	4-F	H	587.8 ± 649
9l	4-Cl	4-Cl	H	403.7 ± 19.6
9m	4-CH_3	4-CH_3	H	261.0 ± 12.5

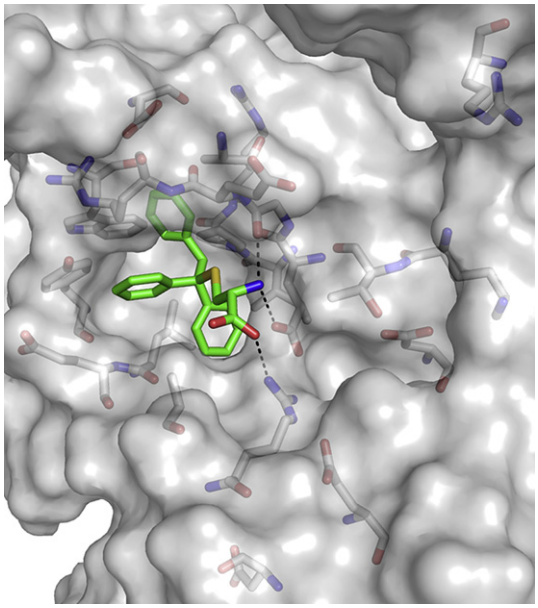

Fig. 3. Docked pose of benzyl STLC analogue **8a**. Hydrogen bonds between the ligand and receptor are marked as dotted lines.

3.5. Determination of multidrug resistance (MDR) ratios

In previous investigations by our group, we uncovered that STLC **4** and related analogues were substrates for the multidrug resistance (MDR) P-glycoprotein (Pgp) cellular efflux pump [16]. This transporter is responsible for the removal of xenobiotics from the cellular environment, with the current antimitotic chemotherapy agents Taxol and the *Vinca* alkaloids among the known substrates [29]. In the case of STLC, the key to molecular recognition by Pgp is the carboxylic acid [16]. While STLC has an MDR ratio of ~30, the thioethanamine without the carboxylate had an MDR ratio of 1, indicating no efflux by Pgp. We examined five of the new benzyl analogues in a Pgp overexpressing cell line, and found the results to be consistent with the previous findings (Table 7). When the acid was present (e.g. **8a**, **8f**, **8g**), the compounds were effluxed from the overexpressing cell line. However, on removal of the acid (e.g. **9f**, **9g**) the MDR ratio returned to 1. Therefore modifications to the trityl head group have little effect on the recognition of STLC and benzyl analogues by Pgp.

4. Conclusions

With the majority of Eg5 inhibitors in the clinical phase of evaluation based around only a handful of scaffolds and thus subject to the same potential liabilities, it is important to develop viable alternatives. STLC and related analogues exhibit strong potential across a number of *in vitro* and *in vivo* cancer models [12,17,30,31]. By quantifying the interactions of STLC with Eg5 for the first time, we have gained a better understanding to guide the development of new analogues of STLC. Towards this end, we modified the trityl region to incorporate a benzyl moiety; activity against Eg5 in the basal ATPase assay was subsequently improved when compared against STLC. Further improvements were also made by introduction of specific substituents to a second phenyl, whilst retaining the benzyl substituent, with a 3-fold gain in

Table 6
Cell line evaluation of benzyl analogues.

Cmpd	Inhibition of basal ATPase activity IC_{50} (nM)	K562 cells GI_{50}[a] [nM]	HCT116 GI_{50}[b] [nM]	NCI-H1299 GI_{50}[c] [nM]	BxPC3 GI_{50}[d] [nM]
4	185.9 ± 20.5	1452 ± 76	553 ± 57	1549 ± 111	1563 ± 155
8c	128.9 ± 15.8	4539 ± 191	n.d.		
8d	67.6 ± 7.4	17,742 ± 3186	n.d.		
9d	256.1 ± 34.6	2729 ± 391	n.d.		
8e	150.5 ± 10.7	6095 ± 587	n.d.		
8h	159.4 ± 15.7	18,239 ± 3565	n.d.		
8k	178.2 ± 19.6	5117 ± 719	n.d.		
8m	106.5 ± 16.1	2786 ± 177	n.d.		
8a	138.0 ± 11.2	3141 ± 296	2371 ± 239	6871 ± 587	14,322 ± 3938
8f	58.6 ± 7.4	2471 ± 360	2084 ± 188	3631 ± 331	3793 ± 643
9f	140.9 ± 16.2	3724 ± 275	2051 ± 270	6792 ± 363	4256 ± 454
8g	167.6 ± 18.1	1442 ± 82	1493 ± 117	2432 ± 263	4335 ± 824
9g	171.9 ± 15.4	2393 ± 215	1170 ± 78	2495 ± 216	4074 ± 550

[a] Human leukaemia (K562).
[b] Lung (NCI-H1299).
[c] Colon (HCT116).
[d] Pancreas (BxPC3) tumour cell lines.

activity realised. Compounds **8d** and **8f** which exhibited the most significantly improved activity were 1:1 mixtures of the (1*R*, 2*R*) and (1*S*, 2*R*) diastereoisomers, and evaluations were based upon the assumption that both compounds were equipotent according to the docking scoring functions. This may not be the case, but problems of separation, combined with no translation of the improvements in activity apparent in the basal assay into the cell growth assays meant further explorations were not pursued. However, our data provides further evidence that the dominant factor that makes STLC a substrate for the P-glycoprotein efflux pump is the carboxylate group in the tail of the molecule. It therefore appears that whilst affinity for Eg5 is largely influenced by the substituent pattern of the head group, the primary drive for Pgp is actually the presence or absence of the carboxylate moiety. Therefore for future development of this series, appropriate replacements for the carboxylate should be identified to address this potential issue. We have used the data from this series of compounds in association with a parallel study to produce a new generation of STLC analogues with improved pharmacodynamic and pharmacokinetic parameters, which will be reported in due course.

5. Experimental section

5.1. Molecular modelling studies

5.1.1. Molecular dynamics (MD) simulations

The crystal structure for the ternary ADP·Eg5·STLC complex in its final bound state (PDB entry 2WOG) was used as the starting structure for all MD simulations [13]. To parameterize the protein, the ff03 force field [32] employed in AMBER [33] was used. For STLC and ADP, hydrogen atoms were added to the crystal structure coordinates, and optimised using the quantum mechanical method HF/6-31G*, followed by a single-point calculation using the same method to determine the electrostatic potential. RESP charges [34] and the specific force field parameters of STLC and ADP were generated using the Antechamber and Parmchk module in AMBER [33]. The complex was solvated in a 270 $Å^3$ box containing 14,515 water molecules and neutralized by adding 5 sodium ions together with 1 chloride ion. For full details of the MD procedures used, see the Supporting Information. The total binding free energies ($\Delta G_{binding}$) for STLC binding with Eg5 were calculated by applying Eq. (1) using the MM/PBSA method [35].

Table 7
Evaluation of benzyl analogues in the PgP overexpressing cell line KB-V1, compared to its isogenic parent cell line KB-3-1.

Cmpd	KB-3-1 GI_{50} [nM]	KB-V1 GI_{50} [nM]	MDR ratio
8a	5333 ± 731	>50,000	>10
8f	4887 ± 1492	>50,000	>10
9f	5546 ± 1403	5781 ± 1016	1
8g	2443 ± 262	>50,000	>20
9g	1884 ± 381	1718 ± 408	1

5.1.2. Docking studies

The crystal structure of Eg5 in complex with STLC (PDB entry 2WOG) was used for docking studies. Chain A of the complex was kept along with waters found less than 3.5 Å away from the protein, ADP and inhibitor atoms. Hydrogen atoms were added to the protein using Accelrys Discovery Studio 2.5 (Accelrys Software, San Diego, USA) and all the inhibitors synthesized within this study docked using GOLD 5.0 for Windows (Cambridge Crystallographic Data Centre, Cambridge, UK). When a compound was prepared as a racemate, both enantiomers were docked. Other than allowing the Chi angles from Ile136, Leu160, Tyr211, Leu214 and Glu215 side chains to deviate ±10° from their crystal values, default software settings were used using Goldscore as a scoring function.

5.1.3. Calculation of physicochemical properties

Physicochemical properties were calculated in Pipeline Pilot 7.4 for Windows (Accelerys Software, San Diego, USA). ALogP and cLogD values are based on the atom based method of Ghose and Cribben [36]. The cLogS values are calculated by the method of Tetko et al. [37].

5.2. Chemistry

All reagents and solvents were of commercial quality and used without further purification. Thin-layer chromatography was carried out on aluminium-backed SiO_2 plates (Merck) and spots visualised using ultra-violet light (254 nm). Compounds were purified by recrystallisation or by flash chromatography using either a Biotage SP4 automated chromatography system or by gravity column chromatography [38]. All chromatography were carried out on SiO_2 60 Å 6–35 μm (Fisher-Scientific). Melting points (Mpt) were determined on Stuart Scientific Melting Point apparatus

SMP1 and are uncorrected. ^{1}H NMR and ^{13}C NMR were run either on a JEOL Lambda Delta 400 (400 MHz), Bruker AMX-400 (400 MHz) or Avance DPX500 (500 MHz) spectrometer. Chemical shifts are stated in parts per million (ppm) and multiplicity indicated as singlet (s), doublet (d), doublet of doublet (dd), triplet (t), quartet (q) and multiplet (m); coupling constants (*J*) are quoted in hertz (Hz). High-resolution mass spectrometry (HRMS) was obtained using electron impact ionisation (ESI, 70 eV) in a Fourier transform analyser by Exactive® Thermo Scientific. Elemental analyses were performed on Perkin Elmer 2400 Analyser Series II elemental analyser. Results for sulphur were obtained by oxygen flask combustion, with hydrogen peroxide as an adsorption solution, and subsequent titration against a solution of barium perchlorate [39]. Infrared spectra for liquid samples were run on Jasco FT-IR-4200 ATR and solid samples compressed with KBr into disks and recorded with Mattson Genesis Series FT-IR spectrometers. Wavenumbers, ν_{max} (cm^{-1}) are quoted for appropriate functional groups. Synthesised compounds were named according to IUPAC nomenclature using ACD ChemSketch 12.01 (Windows, Advanced Chemistry Development, Toronto, Canada). STLC was obtained from Novabiochem.

*5.2.1. General procedure A: synthesis of tertiary alcohols **7a**–**7l***

The required ketone (10 mmol) was added to benzylmagnesium chloride (2 M solution in THF; 10 mL, 20 mmol) under a nitrogen atmosphere at 0 °C and the mixture stirred at room temperature for 24 h. The reaction mixture was then quenched with saturated ammonium chloride (20 mL), extracted with EtOAc (3 × 10 mL), dried ($MgSO_4$) and the solvent was removed under reduced pressure. The crude residue was purified either by recrystallisation or flash chromatography [EtOAc:*n*-hexane (10:90)].

*5.2.1.1. 1,1,2-Triphenylethanol (**7a**).* General procedure A with benzylmagnesium chloride (9.75 mL, 19.5 mmol) and benzophenone (2.73 g, 15 mmol) afforded **7a** after recrystallisation from MeOH as a white solid (2.39 g, 58%). Mpt: 85–87 °C (lit. 87–88 °C) [40]. ^{1}H NMR (400 MHz): δ ($CDCl_3$): 2.32 (1H, s), 3.67 (2H, s), 6.87–6.92 (2H, m), 7.17–7.45 (13H, m). ^{13}C NMR (125 MHz): δ ($CDCl_3$): 48.03, 77.97, 126.27, 126.90, 126.99, 128.17, 130.98, 135.85, 146.64. Elemental analysis: Found C, 87.52; H, 6.44 (Required for $C_{20}H_{18}O$: C, 87.52; H, 6.61). HRMS-ESI (+ve): Calculated for $C_{20}H_{17}$ $(M - OH)^+$ 257.1325, found 257.1322. IR: KBr disc, ν_{max} (cm^{-1}): 3549.7 (–OH stretch of tertiary alcohol).

*5.2.1.2. 1-(2-Fluorophenyl)-1,2-diphenylethanol (**7b**).* General procedure A with 2-fluorobenzophenone (2.00 g, 10 mmol) after recrystallisation from MeOH gave the racemate **7b** (2.00 g, 68%) as a white solid. Mpt: 85–86 °C. ^{1}H NMR (400 MHz): δ ($CDCl_3$): 2.53 (1H, d, J = 3.2 Hz, OH), 3.57 (1H, d, J = 13.4 Hz, CH_2), 3.88 (1H, d, J = 13.2 Hz, CH_2), 6.92–7.30 (14H, m). ^{13}C NMR (125 MHz): δ ($CDCl_3$): 45.98 (d, J_{CF} = 3.9 Hz), 77.31, 116.1 (d, J_{CF} = 23.3 Hz), 124.00 (d, J_{CF} = 3.3 Hz), 126.10, 126.80, 127.40, 127.90 (d, J_{CF} = 4.2 Hz), 128.07, 128.17, 129.3 (d, J_{CF} = 8.5 Hz), 130.84, 133.4 (d, J_{CF} = 11.2 Hz), 136.03, 145.79, 159.72 (d, J_{CF} = 245.4 Hz). HRMS-ESI (+ve): Calculated for $C_{20}H_{16}F$ $(M - OH)^+$ 275.1231, found 275.1232. IR: KBr disc, ν_{max} (cm^{-1}): 3588.3 (–OH stretch of tertiary alcohol).

*5.2.1.3. 1-(3-Chlorophenyl)-1,2-diphenylethanol (**7c**).* General procedure A with benzylmagnesium chloride (5.00 mL, 10 mmol) and 3-chlorobenzophenone (1.08 g, 5 mmol) after flash chromatography gave the racemate **7c** (0.55 g, 36%) as a colourless oil. ^{1}H NMR (400 MHz): δ ($CDCl_3$): 2.32 (1H, s, OH), 3.58–3.66 (2H, m), 6.88–6.91 (2H, m), 7.18–7.42 (12H, m). ^{13}C NMR (125 MHz): δ ($CDCl_3$): 47.86, 77.64, 124.50, 126.14, 126.57, 127.12, 127.30, 128.31, 128.37, 129.40, 130.91, 134.21, 135.33, 146.01, 148.79. HRMS-ESI (+ve): Calculated for $C_{20}H_{16}(^{35}Cl)$ $(M - OH)^+$ 291.0935, found 291.0935. IR: ATR, ν_{max} (cm^{-1}): 3564.6 (–OH stretch of tertiary alcohol).

*5.2.1.4. 3-(1-Hydroxy-1,2-diphenylethyl)phenol (**7d**).* General procedure A with benzylmagnesium chloride (5.00 mL, 10 mmol) and 3-hydroxybenzophenone (0.45 g, 2.27 mmol) after flash chromatography gave the racemate **7d** (0.50 g, 76%) as a colourless oil. ^{1}H NMR (400 MHz): δ ($CDCl_3$): 2.28 (1H, s, OH); 3.58–3.65 (2H, m, CH_2); 4.67 (1H, s, OH), 6.67–6.71 (2H, m), 6.89–7.43 (12H, m). ^{13}C NMR (125 MHz): δ ($CDCl_3$): 47.90, 77.80, 113.54, 113.92, 118.75, 126.17, 126.96, 127.08, 128.21, 129.39, 130.96, 135.72, 146.40, 148.63, 155.44. HRMS-ESI (–ve): Calculated for $C_{20}H_{17}O_2$ $(M - H)^-$ 289.1234, found 289.1235. IR: ATR, ν_{max} (cm^{-1}): 3563.7 (–OH stretch of tertiary alcohol).

*5.2.1.5. 1-(4-Fluorophenyl)-1,2-diphenylethanol (**7e**).* General procedure A with 4-fluorobenzophenone (2.00 g, 10 mmol) after recrystallisation from MeOH gave the racemate **7e** (2.30 g, 79%) as a white solid. Mpt: 78–79 °C. ^{1}H NMR (400 MHz): δ ($CDCl_3$): 2.34 (1H, s, OH), 3.61 (1H, d, J = 13.2 Hz, CH_2), 3.65 (1H, d, J = 13.3 Hz, CH_2), 6.89–6.92 (2H, m), 6.93–7.44 (12H, m). ^{13}C NMR (125 MHz): δ ($CDCl_3$): 48.13, 77.69, 114.89 (d, J_{CF} = 21.4 Hz), 126.23, 127.01, 127.18, 128.08 (d, J_{CF} = 10.5 Hz), 128.24, 128.29, 130.96, 135.65, 142.47 (d, J_{CF} = 3.1 Hz), 146.52, 161.80 (d, J_{CF} = 245.9 Hz). HRMS-ESI (+ve): Calculated for $C_{20}H_{16}F$ $(M - OH)^+$ 275.1231, found 275.1231. IR: KBr disc, ν_{max} (cm^{-1}): 3575.3 (–OH stretch of tertiary alcohol).

*5.2.1.6. 1-(4-Chlorophenyl)-1,2-diphenylethanol (**7f**).* General procedure A with 4-chlorobenzophenone (2.00 g, 9.25 mmol) after flash chromatography gave the racemate **7f** (1.50 g, 53%) as a pale yellow oil. ^{1}H NMR (400 MHz): δ ($CDCl_3$): 2.32 (1H, s, OH), 3.60 (1H, d, J = 13.3 Hz, CH_2), 3.64 (1H, d, J = 13.3 Hz, CH_2), 6.88–6.92 (2H, m), 7.17–7.41 (12H, m). ^{13}C NMR (125 MHz): δ ($CDCl_3$): 47.91, 77.66, 126.17, 127.07, 127.27, 127.79, 128.25, 128.29, 128.34, 130.94, 132.80, 135.48, 145.19, 146.30. HRMS-ESI (+ve): Calculated for $C_{20}H_{16}(^{35}Cl)$ $(M - OH)^+$ 291.0935, found 291.0934. IR: ATR, ν_{max} (cm^{-1}): 3275.9 (–OH stretch of tertiary alcohol).

*5.2.1.7. 1-(4-Methylphenyl)-1,2-diphenylethanol (**7g**).* General procedure A with 4-methylbenzophenone (1.96 g, 10 mmol) after recrystallisation from MeOH gave the racemate **7g** (1.30 g, 46%) as a white solid. Mpt: 80–81 °C (lit. 89 °C) [41]. ^{1}H NMR (400 MHz): δ ($CDCl_3$): 2.25 (1H, s, OH), 2.30 (3H, s, CH_3), 3.60–3.63 (2H, m, CH_2), 6.87–6.93 (2H, m), 7.09–7.40 (12H, m). ^{13}C NMR (100 MHz): δ ($CDCl_3$): 21.08, 48.03, 77.42, 126.17, 126.60, 126.82, 126.85, 128.10, 128.87, 130.99, 136.00, 136.58, 143.80, 146.79. HRMS-ESI (+ve): Calculated for $C_{21}H_{19}O$ $(M - OH)^+$ 271.1481, found 271.1475. IR: KBr disc, ν_{max} (cm^{-1}): 3584.9 (–OH stretch of tertiary alcohol).

*5.2.1.8. 4-(1-Hydroxy-1,2-diphenylethyl)phenol (**7h**).* General procedure A with 4-hydroxybenzophenone (1.98 g, 10 mmol) after recrystallisation from MeOH gave the racemate **7h** (2.50 g, 86%) as a white solid. Mpt: 82–84 °C. ^{1}H NMR (400 MHz): δ ($CDCl_3$): 2.30 (1H, s, OH), 3.59 (2H, s, CH_2), 4.98 (1H, s, OH), 6.72–6.76 (2H, m); 7.15–7.46 (12H, m). ^{13}C NMR (100 MHz): δ ($CDCl_3$): 48.13, 77.84, 114.95, 126.86, 126.92, 127.79, 128.12, 128.13, 129.88, 130.99, 135.93, 139.05, 146.74, 154.50. HRMS-ESI (+ve): Calculated for $C_{20}H_{17}O$ $(M - OH)^+$ 273.1274, found 273.0400. IR: ATR, ν_{max} (cm^{-1}): 3385.9 (–OH stretch of tertiary alcohol).

*5.2.1.9. 1-(3,4-Dichlorophenyl)-1,2-diphenylethanol (**7i**).* General procedure A with 3,4-dichlorobenzophenone (2.50 g, 10 mmol) after flash chromatography gave the racemate **7i** (2.20 g, 64%) as

a colourless oil. ^{1}H NMR (400 MHz): δ ($CDCl_3$): 2.34 (1H, s, OH), 3.57 (1H, d, J = 13.4 Hz, CH_2), 3.64 (1H, d, J = 13.4 Hz, CH_2), 6.89–6.92 (2H, m), 7.18–7.60 (11H, m). ^{13}C NMR (125 MHz): δ ($CDCl_3$): 47.79, 60.55, 125.84, 126.07, 127.25, 127.51, 128.41, 128.46, 128.50, 130.03, 130.88, 130.96, 132.31, 135.07, 145.72, 147.04. HRMS-ESI (+ve): Calculated for $C_{20}H_{15}(^{35}Cl_2)$ $(M - OH)^+$ 325.0545, found 325.0543. IR: ATR, ν_{max} (cm^{-1}): 3475.3 (–OH stretch of tertiary alcohol).

*5.2.1.10. 1,1-Bis(4-fluorophenyl)-2-phenylethanol (**7j**).* General procedure A with 4,4′-difluorobenzophenone (2.18 g, 10 mmol) after recrystallisation from MeOH gave **7j** (1.00 g, 32%) as a white solid. Mpt: 88–89 °C. ^{1}H NMR (400 MHz): δ ($CDCl_3$): 2.32 (1H, s, OH), 3.59 (2H, s, CH_2), 6.86–6.90 (2H, m), 6.97–7.39 (11H, m). ^{13}C NMR (400 MHz): δ ($CDCl_3$): 48.22, 77.37, 115.00 (d, J_{CF} = 21.6 Hz), 127.12, 128.02 (d, J_{CF} = 8.0 Hz), 128.31, 130.90, 135.37, 142.30 (d, J_{CF} = 3.0 Hz), 161.86 (d, J_{CF} = 246.2 Hz). HRMS-ESI (+ve): Calculated for $C_{20}H_{15}F_2$ $(M - OH)^+$ 293.1136, found 293.1138. IR: KBr disc, ν_{max} (cm^{-1}): 3557.3 (–OH stretch of tertiary alcohol).

*5.2.1.11. 1,1-Bis(4-chlorophenyl)-2-phenylethanol (**7k**).* General procedure A with 4,4′-dichlorobenzophenone (2.50 g, 10 mmol) after recrystallisation from MeOH gave **7k** (0.70 g, 20%) as a pale yellow solid. Mpt: 112–113 °C (lit. 116–117 °C) [42]. ^{1}H NMR (400 MHz): δ ($CDCl_3$): 2.31 (1H, s, OH), 3.58 (2H, s, CH_2), 6.87–6.90 (2H, m), 7.18–7.34 (11H, m). ^{13}C NMR (125 MHz): δ ($CDCl_3$): 47.80, 77.32, 127.24, 127.66, 128.41, 130.87, 133.10, 135.05, 144.79. HRMS-ESI (+ve): Calculated for $C_{20}H_{15}(^{35}Cl_2)$ $(M - OH)^+$ 325.0545, found 325.0545. IR: KBr disc, ν_{max} (cm^{-1}): 3528.5 (–OH stretch of tertiary alcohol).

*5.2.1.12. 1,1-Bis(4-methylphenyl)-2-phenylethanol (**7l**).* General procedure A with benzylmagnesium chloride (5.00 mL, 10 mmol) and 4,4′-dimethylbenzophenone (1.05 g, 5 mmol) after flash chromatography gave **7l** (0.90 g, 60%) as a colourless oil. ^{1}H NMR (400 MHz): δ ($CDCl_3$): 2.23 (1H, s, OH), 2.31 (6H, s, 2 × CH_3), 3.60 (2H, s, CH_2), 6.90–6.93 (2H, m), 7.08–7.11 (4H, m), 7.15–7.17 (3H, m), 7.30 (4H, m). ^{13}C NMR (125 MHz): δ ($CDCl_3$): 21.07, 48.04, 77.78, 126.11, 126.76, 128.09, 128.82, 131.02, 136.15, 136.43, 143.95. HRMS-ESI (+ve): Calculated for $C_{22}H_{21}$ $(M - OH)^+$ 285.1638, found 285.1638. IR: ATR, ν_{max} (cm^{-1}): 3566.2 (–OH stretch of tertiary alcohol).

*5.2.1.13. 1-(3-Chlorophenyl)-1-(4-chlorophenyl)-2-phenylethanol (**7m**).* 3-Chlorobromobenzene (0.57 g, 3 mmol) was dissolved in dry THF (5 mL), the solution cooled to −78 °C, *n*-butyllithium (2.7 M solution in heptane; 1.20 mL, 3.30 mmol) added and the mixture stirred for 30 min. A solution of 4-chloro-2-benzophenone (0.69 g, 3.00 mmol) in THF (10 mL) was then added dropwise to the mixture and stirred for a further 24 h. The reaction was quenched with saturated aqueous ammonium chloride (20 mL) and extracted with EtOAc (3 × 20 mL). The combined organic fractions were dried ($MgSO_4$) and the solvent removed under reduced pressure. The crude residue was purified using flash column chromatography [EtOAc:*n*-hexane, (10:90)] to afford the racemate **7m** (0.43 g, 42%) as a colourless liquid. ^{1}H NMR (400 MHz): δ ($CDCl_3$): 2.32 (1H, s, OH), 3.57–3.60 (2H, m, CH_2), 6.87–6.91 (2H, m), 7.18–7.43 (11H, m). ^{13}C NMR (125 MHz): δ ($CDCl_3$): 47.76, 77.32, 124.38, 126.48, 127.31, 127.40, 127.66, 128.46, 129.56, 130.86, 133.16, 134.39, 134.94, 144.54, 148.41. HRMS-ESI (+ve): Calculated for $C_{20}H_{15}(^{35}Cl_2)$ $(M + H - OH)^+$ 325.0545, found 325.0543. Calculated $C_{20}H_{15}(^{35}Cl)(^{37}Cl)$ $(M + H - OH)^+$ 327.0516, found 327.0514. IR: ATR, ν_{max} (cm^{-1}): 3552.2 (–OH stretch of tertiary alcohol).

*5.2.1.14. 1,1,3-Triphenylprop-2-yn-1-ol (**10**).* General procedure A adapted with lithium phenylacetylide (1 M solution in THF; 15 mL, 15 mmol) and benzophenone (1.8 g, 10 mmol) after purification by flash chromatography [EtOAc:*n*-hexane (15:85)] gave **10** (2.0 g, 70%) as a pale yellow solid. Mpt: 76–77 °C (lit. 78–80 °C) [43]. ^{1}H NMR (400 MHz): δ ($CDCl_3$): 2.91 (1H, s, OH), 7.34–7.70 (15H, m). ^{13}C NMR (125 MHz): δ ($CDCl_3$): 74.94, 87.34, 91.79, 122.51, 126.16, 127.85, 128.43, 128.79, 131.89, 145.11. HRMS-ESI (+ve): Calculated for $C_{21}H_{15}$ $(M - OH)^+$ 267.1168, found 267.1166. IR: KBr disc, ν_{max} (cm^{-1}): 3546.4 (–OH stretch of tertiary alcohol).

*5.2.1.15. 2-Hydroxy-1,2,2-triphenylethanone (**13**).* General procedure A adapted with phenyllithium (1.8 M solution in THF; 5 mL, 9 mmol) and benzil (1.05 g, 5 mmol) after purification by flash chromatography [EtOAc:*n*-hexane (20:80)] gave **13** (1.00 g, 35%) as a white solid. Mpt: 78–79 °C (lit. 81–83 °C) [44]. ^{1}H NMR (400 MHz): δ ($CDCl_3$): 4.98 (1H, s, OH), 7.27–7.44 (13H, m), 7.69–7.72 (2H, m). ^{13}C NMR (125 MHz): δ ($CDCl_3$): 85.13, 128.21, 128.24, 128.41, 128.47, 130.92, 133.04, 135.19, 141.98, 200.90. HRMS-ESI (+ve): Calculated for $C_{20}H_{15}O$ $(M - OH)^+$ 271.1117, found 271.1118. IR: KBr disc, ν_{max} (cm^{-1}): 3468.2 (–OH stretch of tertiary alcohol), 1667.9 (C=O stretch of ketone).

*5.2.1.16. 1,1,3-Triphenylpropan-1-ol (**11**).* 1,1,3-Triphenylprop-2-yn-1-ol (**10**, 0.586 g, 2.00 mmol) was dissolved in EtOAc (20 mL) and a mixture of Lindlar's catalyst (0.080 g) and K_2CO_3 (0.080 g, 0.58 mmol) added to the solution. The reaction flask was purged, filled with H_2 gas and the mixture stirred at atmospheric pressure for 72 h at room temperature. The reaction was then filtered and the solvent removed under reduced pressure, and the crude residue was subsequently purified by flash column chromatography [EtOAc:*n*-hexane(10:90)] to give **11** (0.432 g, 73%) as a white solid. Mpt: 85–87 °C (lit. 87–88 °C) [45]. ^{1}H NMR (400 MHz): δ ($CDCl_3$): 2.14 (1H, s, OH), 2.61 (4H, s, 2 × CH_2) 7.15–7.47 (15H, m). ^{13}C NMR (125 MHz): δ ($CDCl_3$): 30.37, 44.09, 78.33, 125.92, 126.10, 127.04, 128.35, 128.48, 128.53, 142.43, 146.90. HRMS-ESI (+ve): Calculated for $C_{21}H_{19}$ $(M - OH)^+$ 271.1481, found 271.1480. IR: KBr disc, ν_{max} (cm^{-1}): 3553.5 (–OH stretch of tertiary alcohol).

5.2.2. General procedure B: preparation of tertiary alcohols via in-situ Grignard generation

Magnesium turnings (0.150 g, 6.17 mmol) were heated to 50 °C for 1 h under a nitrogen atmosphere and two chips of iodine were then added. The reaction mixture was cooled to room temperature, anhydrous Et_2O added (10 mL), followed by a solution of the substituted benzyl bromide derivative (3.00 mmol) in anhydrous Et_2O (10 mL), and the mixture stirred for 3 h. A solution of benzophenone (0.375 g, 2.06 mmol) in anhydrous Et_2O (10 mL) was added and the reaction stirred for a further 24 h under nitrogen at room temperature. The reaction was quenched with saturated aqueous ammonium chloride (20 mL), extracted with EtOAc (3 × 20 mL), the combined organic fractions were dried ($MgSO_4$) and the solvent was removed under reduced pressure. Purification of the crude residue by flash chromatography [EtOAc:*n*-hexane (10:90)] afforded the desired tertiary alcohol product.

*5.2.2.1. 2-(3-Chlorophenyl)-1,1-diphenylethanol (**15a**).* General procedure B with 3-chlorobromobenzyl bromide (0.60 g, 3 mmol) afforded **15a** (0.60 g, 49%) as a white solid. Mpt: 162–163 °C. ^{1}H NMR (400 MHz): δ ($CDCl_3$): 2.25 (1H, s, OH), 3.64 (2H, s, CH_2), 6.74 (1H, d, J = 7.6 Hz), 6.90 (1H, s), 7.05 (1H, t, J = 7.6 Hz), 7.14 (1H, d, J = 7.6 Hz), 7.24–7.40 (10H, m). ^{13}C NMR (100 MHz): δ ($CDCl_3$): 47.75, 78.11, 126.29, 126.91, 127.22, 128.26, 129.10, 133.11, 133.72, 138.25, 146.30. Elemental analysis: Found C, 77.60; H, 5.48 (Required for $C_{20}H_{17}ClO$: C, 77.79; H, 5.55). HRMS-ESI (+ve): Calculated for $C_{20}H_{16}(^{35}Cl)$ $(M + H - OH)^+$ 291.0932, found 291.0935. Calculated for $C_{20}H_{16}(^{37}Cl)$ $(M + H - OH)^+$ 291.0903,

found 293.0906. IR: KBr disc, ν_{max} (cm^{-1}): 3560.4 (−OH stretch of tertiary alcohol).

*5.2.2.2. 2-(4-Chlorophenyl)-1,1-diphenylethanol (**15b**).* General procedure B with 4-chlorobromobenzyl bromide (0.60 g, 3 mmol) afforded **15b** (0.28 g, 30%) as a white solid. Mpt: 115–117 °C (lit. 116 °C) [46]. ^{1}H NMR (400 MHz): δ ($CDCl_3$): 2.20 (1H, s, OH), 3.59 (2H, s, CH_2), 6.79–6.83 (2H, m), 7.09–7.12 (2H, m), 7.22–7.40 (10H, m). ^{13}C NMR (125 MHz): δ ($CDCl_3$): 47.37, 78.03, 126.26, 127.15, 128.12, 128.25, 132.24, 132.73, 134.56, 146.33. Elemental analysis: Found C, 77.43; H, 5.63 (Required for $C_{20}H_{17}ClO$: C, 77.79; H, 5.55). HRMS-ESI (+ve): Calculated for $C_{20}H_{16}(^{35}Cl)$ $(M + H - OH)^+$ 291.0932, found 291.0935. Calculated for $C_{20}H_{16}(^{37}Cl)$ $(M + H - OH)^+$ 291.0903, found 293.0906. IR: KBr disc, ν_{max} (cm^{-1}): 3530.1 (−OH stretch of tertiary alcohol).

*5.2.2.3. 2-(3,4-Dichlorophenyl)-1,1-diphenylethanol (**15c**).* General procedure B with 3,4-dichlorobromobenzyl bromide (0.72 g, 3 mmol) afforded **15c** (0.38 g, 37%) as a white solid. Mpt: 65–66 °C. ^{1}H NMR (400 MHz): δ ($CDCl_3$): 2.17 (1H, s, OH), 3.55 (2H, s, CH_2), 6.67 (1H, dd, J = 2.0, 8.4 Hz), 6.99 (1H, d, J = 2.0 Hz), 7.16 (1H, d, J = 8.4 Hz), 7.16–7.37 (10H, m). ^{13}C NMR (125 MHz): δ ($CDCl_3$): 47.20, 78.13, 126.27, 127.34, 128.31, 129.64, 130.25, 130.73, 131.72, 132.86, 136.66, 146.06. Elemental analysis: Found C, 69.86; H, 4.40 (Required for $C_{20}H_{16}Cl_2O$: C, 69.98; H, 4.70). HRMS-ESI (+ve): $C_{20}H_{15}(^{35}Cl_2)$ $(M + H - OH)^+$ 325.0545, found 325.0543. $C_{20}H_{15}(^{35}Cl)(^{37}Cl)$ $(M + H - OH)^+$ 327.0516, found 327.0514. IR: KBr disc, ν_{max} (cm^{-1}): 3566.9 (−OH stretch of tertiary alcohol).

5.2.3. General procedure C: preparation of L-cysteine thioethers using boron trifluoride diethyl etherate

The procedure reported by DeBonis et al. was used [12]. L-Cysteine (0.058 g, 0.48 mmol) and the required tertiary alcohol (0.48 mmol) were dissolved in acetic acid (0.5 mL). $BF_3 \cdot Et_2O$ (0.09 mL, 0.82 mmol) was added dropwise under a nitrogen atmosphere at 0 °C. The reaction mixture was stirred at 0 °C for 2 h, then quenched with 10% aqueous sodium acetate solution (1.5 mL), followed by H_2O (1.5 mL). The resulting precipitate was filtered, washed with H_2O and Et_2O, and then dried in a vacuum oven (40 °C for 24 h) to give the corresponding L-cysteine derivatives.

*5.2.3.1. 4-((((2R)-2-Ammonio-2-carboxyethyl)sulfanyl)(diphenyl)-methyl)pyridinium tetrafluoroborate (**6**).* General procedure C with diphenyl(pyridin-4-yl)methanol (0.522 g, 2 mmol) and L-cysteine (0.242 g, 2 mmol) gave compound **6** (0.300 g, 28%) as a white solid. Mpt: 164–166 °C. ^{1}H NMR (400 MHz): δ (CD_3OD): 2.74–2.85 (2H, m, CH_2), 3.59 (1H, t, J = 5.2 Hz, CH), 7.29–7.50 (10H, m), 8.19 (2H, d, J = 6.8 Hz), 8.76 (2H, d, J = 6.8 Hz). ^{13}C NMR (125 MHz): δ (DMSO-d_6): 31.60, 51.41, 65.47, 123.92, 127.36, 128.45, 128.88, 128.92, 142.43, 142.52, 149.75, 152.25, 168.87. Elemental analysis: Found: C, 46.31; H, 4.37; N, 5.24 (Required for: $C_{21}H_{22}N_2O_2S \cdot 2BF_4$: C, 46.70; H, 4.11; N, 5.19). HRMS-ESI (+ve): Calculated for $C_{21}H_{21}N_2O_2S$ $(M + H)^+$ 365.1318, found 365.1321. IR: KBr disc, ν_{max} (cm^{-1}): 1635.8 (C=O stretch for carboxylic acid), 3032.1 (OH stretch for carboxylic acid).

*5.2.3.2. (2R)-2-Amino-3-((1,1,2-triphenylethyl)sulfanyl)propanoic acid (**8a**).* General procedure C with 1,1,2-triphenylethanol (**7a**) (0.658 g, 2.4 mmol) and L-cysteine (0.292 g, 2.4 mmol) gave **8a** (0.335 g, 37%) as a white solid. Mpt: 169–170 °C. ^{1}H NMR (400 MHz): δ (DMSO-d_6): 2.34 (1H, dd, J = 9.2, 12.8 Hz, CH_2), 2.61 (1H, dd, J = 12.4, J = 4.0 Hz, CH_2), 2.87 (1H, dd, J = 4.0, 9.2 Hz, CH), 3.63–3.69 (2H, m, CH_2), 6.66–6.70 (2H, m), 6.99–7.31 (13H, m). ^{13}C NMR (125 MHz): δ (DMSO-d_6): 31.21, 40.08, 45.08, 53.51, 61.00, 126.01, 126.54, 126.59, 126.89, 127.65, 127.69, 128.50, 128.75, 130.96, 136.63, 144.31, 144.51, 168.14. Elemental analysis: Found: C, 73.41; H, 5.93; N, 3.81; S, 8.14 (Required for $C_{23}H_{23}NO_2S$: C, 73.18; H, 6.14; N, 3.71; S, 8.49). HRMS-ESI (+ve): Calculated for $C_{23}H_{24}NO_2S$ $(M + H)^+$ 378.1522, found 378.1527. IR: KBr disc, ν_{max} (cm^{-1}): 1617.2 (C=O stretch for carboxylic acid).

*5.2.3.3. (2R)-2-Amino-3-((1-(2-fluorophenyl)-1,2-diphenylethyl)sulfanyl)propanoic acid (**8b**).* General procedure C with 1-(2-fluorophenyl)-1,2-diphenylethanol (**7b**, 0.592 g, 2 mmol) and L-cysteine (0.242 g, 2 mmol) gave **8b** (0.14 g, 19%) as a white solid. Mpt: 160–161 °C. ^{1}H NMR (400 MHz): δ (CD_3OD): 2.54–2.65 (1H, m, CH_2), 2.73–2.79 (1H, m, CH_2), 2.90–3.02 (1H, m, CH), 3.82–3.85 (2H, m, CH_2), 6.80–6.85 (2H, m), 6.97–7.37 (12H, m). ^{13}C NMR (100 MHz): δ (CD_3OD): 42.83, 44.48, 53.61, 59.61, 60.18, 115.80, 115.83, 116.02, 116.05, 123.41, 123.67, 126.10, 126.17, 126.64, 126.71, 126.94, 127.91, 128.00, 129.31, 129.52, 130.49, 131.44, 131.47, 136.27, 136.42, 144.49, 144.82, 156.16, 157.24, 161.47, 162.05, 170.83, 170.87. Elemental analysis: Found: C, 69.37; H, 5.60; N, 3.49; S, 7.95 (Required for $C_{23}H_{22}FNO_2S$: C, 69.85; H, 5.61; N, 3.54; S, 8.11). HRMS-ESI (+ve): Calculated for $C_{23}H_{23}FNO_2S$ $(M + H)^+$ 396.1428, found 396.1427. IR: KBr disc, ν_{max} (cm^{-1}): 1636.0 (C=O stretch for carboxylic acid).

*5.2.3.4. (2R)-2-Amino-3-((1-(3-chlorophenyl)-1,2-diphenylethyl)sulfanyl)propanoic acid (**8c**).* General procedure C with 1-(3-chlorophenyl)-1,2-diphenylethanol (**7c**, 0.275 g, 0.892 mmol) and L-cysteine (0.108 g, 0.892 mmol) afforded **8c** (0.04 g, 11%) as a white solid. Mpt: 152–153 °C. ^{1}H NMR (400 MHz): δ (CD_3OD): 2.56–2.66 (1H, m, CH_2), 2.87–2.93 (1H, m, CH_2), 3.02–3.11 (1H, m, CH); 3.61–3.75 (2H, m, CH_2), 6.69–6.74 (2H, m), 6.99–7.39 (12H, m). ^{13}C NMR (125 MHz): δ (CD_3OD): 32.23, 32.28, 46.45, 46.83, 55.10, 55.19, 62.51, 62.67, 127.46, 128.04, 128.16, 128.25, 128.35, 128.49, 128.79, 129.11, 129.20, 130.01, 130.09, 130.29, 130.37, 130.49, 132.36, 132.39, 134.88, 134.97, 137.45, 145.29, 145.31, 148.12, 172.69. Elemental analysis: Found: C, 61.48; H, 5.79; N, 3.17 (Required for $C_{23}H_{22}ClNO_2S \cdot 2H_2O$: C, 61.67; H, 5.85; N, 3.13). HRMS-ESI (+ve): Calculated for $C_{23}H_{23}(^{35}Cl)NO_2S$ $(M + H)^+$ 412.1133, found 412.1128. Calculated $C_{23}H_{23}(^{37}Cl)NO_2S$ $(M + H)^+$ 414.1103, found 414.1098. IR: KBr disc, ν_{max} (cm^{-1}): 1615.9 (C=O stretch for carboxylic acid).

*5.2.3.5. (2R)-2-Amino-3-((1-(3-hydroxyphenyl)-1,2-diphenylethyl) sulfanyl)propanoic acid (**8d**).* General procedure C with 3-(1-hydroxy-1,2-diphenylethyl)phenol (**7d**, 0.320 g, 1.1 mmol) and L-cysteine (0.133 g, 1.1 mmol) afforded **8d** (0.045 g, 10%) as a white solid. Mpt: 186–187 °C. ^{1}H NMR (400 MHz): δ (CD_3OD): 2.59–2.67 (1H, m, CH_2), 2.89–2.95 (1H, m, CH_2), 3.09–3.06 (1H, m, CH); 3.65–3.68 (2H, m, CH_2), 6.69–7.37 (14H, m). ^{13}C NMR (100 MHz): δ (CD_3OD): 32.09, 46.87, 47.01, 55.09, 55.11, 62.83, 114.89, 114.97, 117.31, 117.62, 121.24, 121.58, 127.27, 127.90, 128.00, 128.04, 128.82, 128.93, 129.80, 129.92, 130.05, 130.40, 132.36, 137.83, 137.86, 145.81, 145.91, 147.24, 147.46, 158.08, 158.18, 172.59. Elemental analysis: Found: C, 67.94; H, 6.08; N, 3.45; S, 8.02 (Required for $C_{23}H_{23}NO_3S \cdot {}^2/_3\ H_2O$: C, 68.14; H, 6.05; N, 3.46; S, 7.91). HRMS-ESI (−ve): Calculated for $C_{23}H_{22}NO_3S$ $(M - H)^-$ 392.1326, found 392.1324. IR: KBr disc, ν_{max} (cm^{-1}): 1598.6 (C=O stretch for carboxylic acid).

*5.2.3.6. (2R)-2-Amino-3-((1-(4-fluorophenyl)-1,2-diphenylethyl)sulfanyl)propanoic acid (**8e**).* General procedure C with 1-(4-fluorophenyl)-1,2-diphenylethanol (**7e**, 0.592 g, 2 mmol) and L-cysteine (0.242 g, 2 mmol) afforded **8e** (0.090 g, 12%) as a white solid. Mpt: 171–172 °C. ^{1}H NMR (400 MHz): δ (CD_3OD): 2.58–2.64 (1H, m, CH_2), 2.86–2.89 (1H, m, CH_2), 2.98–3.04 (1H, m, CH), 3.62–3.75 (2H, m, CH_2), 6.68–6.72 (2H, m), 6.95–7.38 (12H, m). ^{13}C NMR (125 MHz): δ (CD_3OD): 32.15, 47.03, 47.31, 55.21, 55.26, 62.63,

62.72, 115.47, 115.59, 115.64, 115.76, 127.52, 128.28, 128.36, 129.16, 129.27, 130.12, 130.45, 132.07, 132.13, 132.47, 132.53, 137.80, 141.69, 142.06, 145.83, 145.89, 162.15, 162.21, 164.10. Elemental analysis: Found: C, 69.40; H, 5.45; N, 3.32; S, 7.79 (Required for $C_{23}H_{22}FNO_2S \cdot {}^1/_5\ H_2O$, C, 69.22; H, 5.66; N, 3.51; S, 8.03). HRMS-ESI (+ve): Calculated for $C_{23}H_{23}FNO_2S$ $(M + H)^+$ 396.14283, found 96.1429. IR: KBr disc, ν_{max} (cm^{-1}): 1603.7 (C=O stretch for carboxylic acid).

*5.2.3.7. (2R)-2-Amino-3-((1-(4-chlorophenyl)-1,2-diphenylethyl)sulfanyl)propanoic acid (**8f**).* General procedure C with 1-(4-chlorophenyl)-1,2-diphenylethanol (**7f**, 0.750 g, 2.43 mmol) and L-cysteine (0.296 g, 2.43 mmol) afforded **8f** (0.290 g, 29%) as a white solid. Mpt: 165–166 °C. ^{1}H NMR (400 MHz): δ (CD_3OD): 2.60–2.65 (1H, m, CH_2), 2.86–2.90 (1H, m, CH_2), 3.01–3.30 (1H, m, CH) 3.64–3.70 (2H, m, CH_2), 6.67–6.74 (2H, m), 6.96–7.37 (12H, m). ^{13}C NMR (100 MHz): δ (CD_3OD): 31.96, 46.68, 46.95, 54.99, 55.03, 62.51, 62.60, 127.43, 128.18, 128.27, 128.87, 128.98, 129.05, 129.15, 129.97, 130.29, 131.70, 132.09, 132.35, 132.38, 132.47, 133.79, 133.86, 137.52, 144.45, 144.77, 145.33, 145.40, 172.22. Elemental analysis: Found: C, 65.96; H, 5.39; N, 3.32; S, 7.95 (Required for $C_{23}H_{22}ClNO_2S \cdot {}^1/_3\ H_2O$: C, 66.11; H, 5.47; N, 3.35; S, 7.92). HRMS-ESI (+ve): Calculated for $C_{23}H_{23}(^{35}Cl)NO_2S$ $(M + H)^+$ 412.1133, found 412.1130. Calculated $C_{23}H_{23}(^{37}Cl)NO_2S$ $(M + H)^+$ 414.1103, found 414.1100. IR: KBr disc, ν_{max} (cm^{-1}): 1615.3 (C=O stretch for carboxylic acid).

*5.2.3.8. (2R)-2-Amino-3-((1-(4-methylphenyl)-1,2-diphenylethyl) sulfanyl)propanoic acid (**8g**).* General procedure C with 1-(4-methylphenyl)-1,2-diphenylethanol (**7g**) (0.272 g, 0.94 mmol) and L-cysteine (0.113 g, 0.94 mmol) afforded **8g** (0.200 g, 21%) as a white solid. Mpt: 148–149 °C. ^{1}H NMR (400 MHz): δ (CD_3OD): 2.30–2.32 (3H, m, CH_3), 2.59–2.62 (1H, m, CH_2), 2.90–2.92 (2H, m), 3.64–3.68 (2H, m, CH_2), 6.63–6.70 (2H, m), 6.93–7.37 (12H, m). ^{13}C NMR (125 MHz): δ (CD_3OD): 20.99, 31.98 46.87, 46.99, 55.10, 62.80, 62.84, 127.25, 127.90, 128.00, 128.04, 128.80, 128.93, 129.51, 129.64, 129.96, 130.04, 130.30, 130.42, 132.38, 137.80, 137.90, 142.87, 142.96, 145.78, 146.00, 172.38. Elemental analysis: Found: C, 72.65; H, 6.18; N, 3.26; S, 8.09 (Required for $C_{24}H_{25}NO_2S \cdot {}^1/_3\ H_2O$: C, 72.52; H, 6.51; N, 3.52; S, 8.19). HRMS-ESI (+ve): Calculated for $C_{24}H_{26}NO_2S$ $(M + H)^+$ 392.1679, found 392.1682. IR: KBr disc, ν_{max} (cm^{-1}): 1608.0 (C=O stretch for carboxylic acid).

*5.2.3.9. (2R)-2-Amino-3-((1-(4-hydroxyphenyl)-1,2-diphenylethyl) sulfanyl)propanoic acid (**8h**).* General procedure C with 1-(4-hydroxyphenyl)-1,2-diphenylethanol (**7h**, 0.870 g, 3 mmol) and L-cysteine (0.360 g, 3 mmol) afforded **8h** (0.090 g, 8%) as a white solid. Mpt: 170–171 °C. ^{1}H NMR (400 MHz): δ (CD_3OD): 2.55–2.60 (1H, m, CH_2), 2.91–2.93 (2H, m), 3.63–3.65 (2H, m, CH_2), 6.68–7.23 (14H, m). ^{13}C NMR (100 MHz): δ (CD_3OD): 30.64, 30.70, 45.72, 45.93, 53.80, 61.35, 61.42, 114.21, 114.34, 125.88, 126.50, 126.60, 126.70, 127.43, 127.56, 128.70, 129.11, 129.87, 130.21, 131.07, 135.17, 135.30, 136.69, 143.42, 144.58, 144.89, 156.08, 156.17, 171.10. Elemental analysis: Found: C, 66.00; H, 6.27; N, 3.22; S, 8.00 (Required for $C_{23}H_{23}NO_3S \cdot H_2O$: C, 66.26; H, 6.19; N, 3.36; S, 7.69). HRMS-ESI (+ve): Calculated for $C_{23}H_{24}NO_3S$ $(M + H)^+$ 394.1471, found 394.1470. IR: KBr disc, ν_{max} (cm^{-1}): 1614.1 (C=O stretch for carboxylic acid).

*5.2.3.10. (2R)-2-Amino-3-((1-(3,4-dichlorophenyl)-1,2-diphenylethyl) sulfanyl)propanoic acid (**8i**).* General procedure C with 1-(3,4-dichlorophenyl)-1,2-diphenylethanol (**7i**, 0.668 g, 2 mmol) and L-cysteine (0.242 g, 2 mmol) afforded **8i** (0.119 g, 13%) as a white solid. Mpt: 163–164 °C. ^{1}H NMR (400 MHz): δ (CD_3OD): 2.60–2.67 (1H, m, CH_2), 2.84–2.94 (1H, m, CH_2), 3.08–3.18 (1H, m, CH), 3.61–3.74 (2H, m, CH_2), 6.72–6.76 (2H, m), 7.02–7.45 (11H, m). ^{13}C NMR (100 MHz): δ (CD_3OD): 30.66, 30.68, 44.99, 45.51, 53.64, 53.72, 60.86, 61.05, 126.27, 126.95, 127.11, 127.20, 127.92, 127.99, 128.63, 128.67, 128.91, 129.03, 129.48, 129.57, 130.50, 130.58, 130.73, 131.01, 131.06, 131.13, 131.46, 131.56, 135.89, 135.92, 143.45, 143.49, 145.15, 145.57, 170.79, 170.84. Elemental analysis: Found: C, 61.37; H, 4.80; N, 3.07; S, 7.01 (Required for $C_{23}H_{21}Cl_2NO_2S \cdot {}^1/_4H_2O$: C, 61.27; H, 4.81; N, 3.11; S, 7.11). HRMS-ESI (+ve): Calculated for $C_{23}H_{22}(^{35}Cl_2)NO_2S$ $(M + H)^+$ 446.0743, found 446.0739. Calculated $C_{23}H_{22}(^{35}Cl)(^{37}Cl)NO_2S$ $(M + H)^+$ 448.0713, found 448.0707. IR: KBr disc, ν_{max} (cm^{-1}): 1617.3 (C=O stretch for carboxylic acid).

*5.2.3.11. (2R)-2-Amino-3-((1-(3-chlorophenyl)-1-(4-chlorophenyl)-2-phenylethyl)sulfanyl)propanoic acid (**8j**).* General procedure C with 1-(3-chlorophenyl)-1-(4-chlorophenyl)-2-phenylethanol (**7m**, 0.340 g, 1.25 mmol) and L-cysteine (0.151 g, 1.25 mmol) afforded **8j** (0.083 g, 15%) as a white solid. Mpt: 163–164 °C. ^{1}H NMR (400 MHz): δ (CD_3OD): 2.58–2.68 (1H, m, CH_2); 2.85–2.91 (1H, m, CH_2), 3.16–3.21 (1H, m, CH), 3.62–3.72 (2H, m, CH_2), 6.72–6.75 (2H, m), 7.02–7.37 (11H, m). ^{13}C NMR (125 MHz): δ (CD_3OD): 32.16, 46.69, 55.20, 55.34, 62.34, 62.41, 127.76, 128.43, 128.51, 128.59, 128.85, 129.27, 129.35, 130.14, 130.49, 130.60, 130.69, 131.81, 132.12, 132.51, 134.27, 134.34, 135.22, 135.29, 137.32, 144.10, 144.23, 147.78, 148.01, 172.22. Elemental analysis: Found: C, 60.89; H, 4.69; N, 3.00; S, 6.98 (Required for $C_{23}H_{21}Cl_2NO_2S \cdot {}^1/_3\ H_2O$: C, 61.07; H, 4.83; N, 3.10; S, 7.09). HRMS-ESI (+ve): Calculated for $C_{23}H_{22}(^{35}Cl_2)NO_2S$ $(M + H)^+$ 446.0743, found 446.0740. Calculated $C_{23}H_{22}(^{35}Cl)(^{37}Cl)NO_2S$ $(M + H)^+$ 448.0713, found 448.0709. IR: KBr disc, ν_{max} (cm^{-1}): 1617.3 (C=O stretch for carboxylic acid).

*5.2.3.12. (2R)-2-Amino-3-((1,1-bis(4-fluorophenyl)-2-phenylethyl) sulfanyl)propanoic acid (**8k**).* General procedure C with 1,1-bis(4-fluorophenyl)-2-phenylethanol (**7j**, 0.700 g, 2.25 mmol) and L-cysteine (0.273 g, 2.25 mmol) afforded **8k** (0.090 g, 10%) as a white solid. Mpt: 168–170 °C. ^{1}H NMR (400 MHz): δ (CD_3OD): 2.60 (1H, dd, J = 9.2, 13.2 Hz, CH_2), 2.86 (1H, dd, J = 4.0, 13.2 Hz, CH_2), 3.09 (1H, dd, J = 3.6, 9.2 Hz, CH), 3.63 (1H, d, J = 13.5 Hz, CH_2), 3.65 (1H, d, J = 13.5 Hz, CH_2), 6.70–6.74 (2H, m), 6.97–7.37 (11H, m). ^{13}C NMR (125 MHz): δ (CD_3OD): 32.06, 47.15, 55.10, 62.05, 115.47, 115.57, 115.64, 115.74, 127.48, 128.22, 131.87, 131.93, 132.22, 132.28, 132.37, 137.51, 141.48, 141.73, 162.06, 162.11, 164.01, 164.07, 172.15. Elemental analysis: Found: C, 63.69; H, 5.38; N, 3.22; S, 7.12 (Required for $C_{23}H_{21}F_2NO_2S \cdot H_2O$: C, 64.02; H, 5.37; N, 3.25; S, 7.43). HRMS-ESI (+ve): Calculated for $C_{23}H_{22}F_2NO_2S$ $(M + H)^+$ 414.1334, found 414.1333. IR: KBr disc, ν_{max} (cm^{-1}): 1603.7 (C=O stretch for carboxylic acid).

*5.2.3.13. (2R)-2-Amino-3-((1,1-bis(4-chlorophenyl)-2-phenylethyl) sulfanyl)propanoic acid (**8l**).* General procedure C with 1,1-bis(4-chlorophenyl)-2-phenylethanol (**7k**, 0.342 g, 1 mmol) and L-cysteine (0.121 g, 1 mmol) afforded **8l** (0.087 g, 20%) as a white solid. Mpt: 170–171 °C. ^{1}H NMR (400 MHz): δ (CD_3OD): 2.62 (1H, dd, J = 9.2, 13.2 Hz, CH_2), 2.87 (1H, dd, J = 3.6, 13.2 Hz, CH_2), 3.15 (1H, dd, J = 4.0, 9.2 Hz, CH), 3.64 (1H, d, J = 13.4 Hz, CH_2), 3.70 (1H, d, J = 13.5 Hz, CH_2), 6.72–6.76 (2H, m), 7.01–7.32 (11H, m). ^{13}C NMR (125 MHz): δ (CD_3OD): 30.67, 45.43, 53.66, 60.81, 126.64, 126.96, 127.72, 127.81, 130.31, 130.65, 131.03, 132.68, 132.75, 135.93, 142.70, 142.92, 170.75. Elemental analysis: Found: C, 61.78; H, 4.54; N, 2.87; S, 6.91 (Required for $C_{23}H_{21}Cl_2NO_2S$: C, 61.88; H, 4.74; N, 3.14; S, 7.18). HRMS-ESI (+ve): Calculated for $C_{23}H_{22}(^{35}Cl_2)NO_2S$ $(M + H)^+$ 446.0743, found 446.0739. Calculated $C_{23}H_{22}(^{35}Cl)(^{37}Cl)NO_2S$ $(M + H)^+$ 448.0713, found 448.0708. IR: KBr disc, ν_{max} (cm^{-1}): 1618.3 (C=O stretch for carboxylic acid).

*5.2.3.14. (2R)-2-Amino-3-((1,1-bis(4-methylphenyl)-2-phenylethyl) sulfanyl)propanoic acid (**8m**).* General procedure C with 1,1-bis(4-methylphenyl)-2-phenylethanol (**7l**, 0.302 g, 1 mmol) and L-cysteine (0.121 g, 1 mmol) afforded **8m** (0.060 g, 15%) as a white solid. Mpt: 162–164 °C. ^{1}H NMR (400 MHz): δ (CD_3OD): 2.30 (3H, s, CH_3), 2.31 (3H, s, CH_3), 2.56–2.62 (1H, m), 2.89–2.96 (2H, m), 3.57–3.72 (2H, m, CH_2), 6.66–6.71 (2H, m), 6.96–7.25 (11H, m). ^{13}C NMR (100 MHz): δ (CD_3OD): 19.65, 19.68, 30.70, 45.61, 53.76, 61.28, 125.88, 126.70, 128.10, 128.24, 128.61, 128.97, 131.07, 136.36, 136.48, 136.67, 141.56, 141.71, 171.19. Elemental analysis: Found: C, 72.19; H, 6.55; N, 3.36; S, 7.84 (Required for $C_{25}H_{27}NO_2S\cdot\frac{1}{2}H_2O$: C, 72.43; H, 6.81; N, 3.38; S, 7.73). HRMS-ESI (−ve): Calculated for $C_{25}H_{26}NO_2S$ $(M-H)^-$ 404.1690, found 404.1694. IR: KBr disc, ν_{max} (cm^{-1}): 1616.3 (C=O stretch for carboxylic acid).

*5.2.3.15. (2R)-2-Amino-3-[(1,1,3-triphenylpropyl)sulfanyl]propanoic acid (**12**).* General procedure C with 1,1,3-triphenylpropan-1-ol (**11**, 0.422 g, 1.46 mmol) and L-cysteine (0.176 g, 1.46 mmol) afforded **12** (0.25 g, 46%) a white solid. Mpt: 170–172 °C. ^{1}H NMR (400 MHz): δ (CD_3OD): 2.38–2.47 (2H, m, CH_2), 2.59–2.71 (3H, m), 2.85–2.89 (1H, m), 3.01–3.05 (1H, dd, m), 7.07–7.47 (15H, m). ^{13}C NMR (100 MHz): δ (CD_3OD): 31.68, 32.12, 48.33, 52.81, 53.70, 126.41, 126.60, 126.72, 126.86, 127.21, 127.55, 127.84, 128.84, 129.00, 138.20, 139.73, 170.08. Elemental analysis: Found: C, 73.29; H, 6.03; N, 3.07; S, 8.02 (Required for $C_{24}H_{25}NO_2S$: C, 73.62; H, 6.44; N, 3.58; S, 8.19). HRMS-ESI (+ve): Calculated for $C_{24}H_{26}NO_2S$ $(M+H)^+$ 392.1679, found 392.1676. IR: KBr disc, ν_{max} (cm^{-1}): 1628.9 (C=O stretch for carboxylic acid).

*5.2.3.16. (2R)-2-Amino-3-((2-oxo-1,1,2-triphenylethyl)sulfanyl)propanoic acid (**14**).* General procedure C with 2-hydroxy-1,2,2-triphenylethanone (**13**, 0.100 g, 1.1 mmol) and L-cysteine (0.042 g, 0.347 mmol) afforded **14** (0.060 g, 44%) as a pale yellow solid. Mpt: 85–86 °C. ^{1}H NMR (400 MHz): δ (CD_3OD): 2.61–2.67 (1H, m, CH_2), 2.69–2.71 (1H, m, CH_2), 3.45–4.47 (1H, m, CH), 7.19–7.54 (13H, m), 7.66–7.68 (2H, m). ^{13}C NMR (125 MHz): δ (CD_3OD): 32.97, 53.86, 71.87, 127.53, 127.70, 128.35, 128.46, 129.03, 129.58, 130.42, 132.16, 136.21, 139.29, 139.71, 174.03, 197.31. Elemental analysis: Found: C, 70.98; H, 5.41; N, 3.60; S, 7.98 (Required for $C_{23}H_{21}NO_3S$: C, 70.56; H, 5.41; N, 3.58; S, 8.19). HRMS-ESI (+ve): Calculated for $C_{23}H_{22}NO_3S$ $(M+H)^+$ 392.1315, found 392.1317. IR: KBr disc, ν_{max} (cm^{-1}): 1627.4 (C=O stretch for carboxylic acid), 1680.3 (C=O stretch for ketone).

*5.2.3.17. (2R)-2-Amino-3-((2-(3-chlorophenyl)-1,1-diphenylethyl) sulfanyl)propanoic acid (**16a**).* General procedure C with 2-(3-chlorophenyl)-1,1-diphenylethanol (**15a**, 0.600 g, 1.94 mmol) and L-cysteine (0.235 g, 1.94 mmol) afforded after flash chromatography [MeOH:CH_2Cl_2 (10:90)] **16a** (0.190 g, 24%) as a white solid. Mpt: 160–161 °C. ^{1}H NMR (400 MHz): δ (CD_3OD): 2.59–2.64 (1H, m, CH_2), 2.89–2.95 (2H, m), 3.65–3.75 (2H, m, CH_2), 6.58 (1H, s), 6.68 (1H, d, J = 7.6 Hz), 6.99 (1H, t, J = 7.6 Hz), 7.06 (1H, d, J = 7.6 Hz), 7.25–7.40 (10H, m). ^{13}C NMR (100 MHz): δ (CD_3OD): 30.58, 45.15, 53.71, 61.41, 126.05, 126.85, 126.93, 127.67, 127.79, 128.12, 128.64, 129.01, 129.51, 130.88, 132.52, 138.84, 144.20, 144.34, 170.92. Elemental analysis: Found: C, 65.92; H, 5.26; N, 3.69; S, 7.47 (Required for $C_{23}H_{22}ClNO_2S\cdot\frac{1}{3}H_2O$: C, 66.11; H, 5.47; N, 3.35; S, 7.47). HRMS-ESI (+ve): Calculated for $C_{23}H_{23}(^{35}Cl)NO_2S$ $(M+H)^+$ 412.1127, found 412.1133. Calculated $C_{23}H_{23}(^{37}Cl)NO_2S$ $(M+H)^+$ 414.1103, found 414.1098. IR: KBr disc, ν_{max} (cm^{-1}): 1617.3 (C=O stretch for carboxylic acid).

*5.2.3.18. (2R)-2-Amino-3-((2-(4-chlorophenyl)-1,1-diphenylethyl) sulfanyl)propanoic acid (**16b**).* General procedure C with 2-(4-chlorophenyl)-1,1-diphenylethanol (**15b**, 0.275 g, 0.89 mmol) and L-cysteine (0.108 g, 0.89 mmol) afforded **16b** (0.082 g, 22%) as a white solid. Mpt: 163–165 °C. ^{1}H NMR (400 MHz): δ (CD_3OD): 2.63 (1H, dd, J = 9.6, 13.2 Hz, CH_2), 2.90 (1H, dd, J = 4.0, 13.2 Hz, CH_2), 2.99 (1H, dd, J = 4.0, 9.6 Hz, CH), 3.68 (2H, dd, J = 13.6 Hz, CH_2), 6.65–6.67 (2H, m), 6.97–6.99 (2H, m), 7.24–7.38 (10H, m). ^{13}C NMR (100 MHz): δ (CD_3OD): 30.58, 44.55, 53.69, 61.39, 126.74, 126.86, 127.64, 127.78, 128.62, 128.98, 132.00, 132.57, 135.34, 144.40, 144.47, 171.03. Elemental analysis: Found: C, 67.14; H, 5.38; N, 3.25; S, 7.39 (Required for $C_{23}H_{22}ClNO_2S$: C, 67.06; H, 5.38; N, 3.40; S, 7.78). HRMS-ESI (+ve): Calculated for $C_{23}H_{23}(^{35}Cl)NO_2S$ $(M+H)^+$ 412.1127, found 412.1133. Calculated $C_{23}H_{23}(^{37}Cl)NO_2S$ $(M+H)^+$ 414.1103, found 414.1098. IR: KBr disc, ν_{max} (cm^{-1}): 1612.1 (C=O stretch for carboxylic acid).

*5.2.3.19. (2R)-2-Amino-3-((2-(3,4-chlorophenyl)-1,1-diphenylethyl) sulfanyl)propanoic acid (**16c**).* General procedure C with 2-(3,4-dichlorophenyl)-1,1-diphenylethanol (**15c**, 0.375 g, 1.1 mmol) and L-cysteine (0.133 mg, 1.1 mmol) afforded **16c** (0.100 g, 20%) as a white solid. Mpt: 162–164 °C. ^{1}H NMR (400 MHz): δ (CD_3OD): 2.62 (1H, dd, J = 9.2, 13.2 Hz, CH_2), 2.88–3.00 (2H, m), 3.65 (1H, d, J = 13.5 Hz, CH_2), 3.72 (1H, d, J = 13.4 Hz, CH_2), 6.66–6.73 (2H, m), 7.14–7.18 (1H, m), 7.25–7.38 (10H, m). ^{13}C NMR (100 MHz): δ (CD_3OD): 30.49, 44.40, 53.64, 61.24, 126.94, 127.02, 127.74, 127.87, 128.56, 128.66, 128.93, 129.66, 130.41, 130.98, 132.80, 137.43, 144.13, 144.21, 170.83. Elemental analysis: Found: C, 61.65; H, 4.87; N, 3.02; S, 7.09 (Required for $C_{23}H_{21}Cl_2NO_2S$: C, 61.88; H, 4.74; N, 3.14; S, 7.18). HRMS-ESI (+ve): Calculated for $C_{23}H_{22}(^{35}Cl_2)NO_2S$ $(M+H)^+$ 446.0743, found 446.0739. Calculated $C_{23}H_{22}(^{35}Cl)(^{37}Cl)NO_2S$ $(M+H)^+$ 448.0713, found 448.0708. IR: KBr disc, ν_{max} (cm^{-1}): 1628.3 (C=O stretch for carboxylic acid).

5.2.4. General procedure D: preparation of cysteamine thioethers using boron trifluouride diethyl etherate

An adaptation of the procedure reported by DeBonis et al. was employed [12]. Cysteamine hydrochloride (54.2 mg, 0.48 mmol) and the requisite tertiary alcohol (0.48 mmol) were dissolved in acetic acid (0.5 mL). $BF_3\cdot Et_2O$ (0.82 mmol) was then added slowly by dropwise addition at 0 °C under nitrogen and stirred for 2 h. The reaction mixture was quenched with 10% aqueous sodium acetate solution (1.5 mL), followed by H_2O (1.5 mL), neutralised with saturated aqueous Na_2CO_3 solution (10 mL) and extracted with EtOAc (3 × 20 mL). The combined organic fractions were dried ($MgSO_4$) and the solvent removed under reduced pressure. The crude residue was then purified unless otherwise noted by flash column chromatography [MeOH:CH_2Cl_2 (10:90)].

*5.2.4.1. 2-((1,1,2-Triphenylethyl)sulfanyl)ethanaminium tetrafluoroborate (**9a**).* General procedure D with 1,1,2-triphenylethanol (**7a**, 0.754 g, 2.75 mmol) and cysteamine hydrochloride (0.310 g, 2.75 mmol) afforded after trituration with Et_2O **9a** (0.335 g, 29%) as a white solid. Mpt: 201–202 °C. ^{1}H NMR (400 MHz): δ (CD_3OD): 2.41 (2H, t, J = 7.6 Hz, CH_2), 2.57 (2H, t, J = 7.6 Hz, CH_2), 3.69 (2H, s, CH_2), 6.63–6.68 (2H, m), 6.98–7.33 (13H, m). ^{13}C NMR (125 MHz): δ (DMSO-d_6): 26.74, 38.45, 45.68, 61.81, 126.71, 127.49, 128.92, 131.32, 136.35, 144.14. Elemental analysis: Found: C, 68.08; H, 6.46; N, 3.76; S, 7.96 (Required for $C_{22}H_{24}NS\cdot BF_4$: C, 68.35; H, 6.26; N, 3.62; S, 8.29). HRMS-ESI (+ve): Calculated for $C_{22}H_{24}NS$ $(M+H)^+$ 334.1624, found 334.1618.

*5.2.4.2. 2-((1-(2-Fluorophenyl)-1,2-diphenylethyl)sulfanyl)ethanamine (**9b**).* General procedure D with 1-(2-fluorophenyl)-1,2-diphenylethanol (**7b**, 1.00 g, 3.42 mmol) and cysteamine hydrochloride (0.386 g, 3.42 mmol) afforded the racemate **9b** (0.143 g, 12%) as a pale yellow gum. ^{1}H NMR (400 MHz): δ ($CDCl_3$): 2.22–2.45

(4H, m, CH_2), 3.66–3.85 (2H, m), 6.77–6.82 (2H, m), 6.97–7.49 (12H, m). ^{13}C NMR (100 MHz): δ ($CDCl_3$): 31.83, 40.19, 44.59, 59.95, 116.36 (d, J_{CF} = 23.3 Hz), 123.77, 126.60, 126.96, 127.17, 127.35, 128.18, 129.51 (d, J_{CF} = 8.9 Hz), 129.96 (d, J_{CF} = 10.2 Hz), 130.96, 131.29, 136.41, 144.81, 160.69 (d, J_{CF} = 248.9 Hz). Elemental analysis: Found: C, 70.42; H, 5.82; N, 3.50; (Required for $C_{22}H_{22}FNS \cdot {}^1/_3 CH_2Cl_2$: C, 70.67; H, 6.02; N, 3.69). HRMS-ESI (+ve): Calculated for $C_{22}H_{23}FNS$ $(M + H)^+$ 352.1530, found 352.1530. IR: ATR, ν_{max} (cm^{-1}): 3410.4 (NH stretch for primary amine).

*5.2.4.3. 2-((1-(3-Chlorophenyl)-1,2-diphenylethyl)sulfanyl)ethanaminium tetrafluoroborate (**9c**).* General procedure D with 1-(3-chlorophenyl)-1,2-diphenylethanol (**7c**, 0.275 g, 0.890 mmol) and cysteamine hydrochloride (0.101 g, 0.892 mmol) afforded the racemate **9c** (0.070 g, 21%) as a pale yellow gum. ^{1}H NMR (400 MHz): δ ($CDCl_3$): 1.80 (2H, s, NH_2), 2.38 (2H, t, J = 6.4 Hz, CH_2), 2.49 (2H, t, J = 6.8 Hz, CH_2), 3.53–3.63 (2H, m, CH_2), 6.62–6.67 (2H, m), 7.04–7.29 (12H, m). ^{13}C NMR (100 MHz): δ ($CDCl_3$): 32.05, 40.17, 46.60, 61.28, 126.70, 127.13, 127.22, 127.33, 128.09, 128.97, 129.08, 129.18, 131.11, 133.87, 135.95, 143.94, 146.80. Elemental analysis: Found: C, 67.65; H, 5.79; N, 3.64; (Required for $C_{22}H_{22}ClNS \cdot {}^1/_4 BF_4$: C, 67.82; H, 5.69; N, 3.59). HRMS-ESI (+ve): Calculated for $C_{22}H_{23}(^{35}Cl)NS$ $(M + H)^+$ 368.1234, found 368.12331. Calculated for $C_{22}H_{23}(^{37}Cl)NS$ $(M + H)^+$ 370.1198, found 370.1205. IR: KBr disc, ν_{max} (cm^{-1}): 3459.1 (NH stretch for primary amine).

*5.2.4.4. 2-((1-(3-Hydroxyphenyl)-1,2-diphenylethyl)sulfanyl)ethanamine (**9d**).* General procedure D with 3-(1-hydroxy-1,2-diphenylethyl)phenol (**7d**, 0.150 g, 0.861 mmol) and cysteamine hydrochloride (0.097 g, 0.861 mmol) gave the racemate **9d** (0.030 g, 10%) as a white solid. Mpt: 160–161 °C. ^{1}H NMR (400 MHz): δ (CD_3OD): 2.44 (2H, t, J = 6.4 Hz, CH_2), 2.52 (2H, t, J = 6.4 Hz, CH_2), 3.62–3.64 (2H, m, CH_2), 6.65–6.70 (3H, m), 6.77–6.83 (2H, m), 6.97–7.32 (9H, m). ^{13}C NMR (100 MHz): δ (CD_3OD): 28.33, 39.03, 45.86, 61.43, 113.55, 116.18, 120.06, 125.99, 126.61, 126.69, 127.48, 128.46, 128.90, 130.97, 136.54, 144.66, 146.27, 156.82. Elemental analysis: Found: C, 67.92; H, 6.13; N, 3.84 (Required for $C_{22}H_{23}NOS \cdot {}^3/_5 CH_2Cl_2$: C, 67.79; H, 6.09; N, 3.50). HRMS-ESI (−ve): Calculated for $C_{22}H_{22}NOS$ $(M - H)^-$ 348.1428, found 348.1428. IR: KBr disc, ν_{max} (cm^{-1}): 3326.5 (OH phenol), 3457.2 (NH stretch for primary amine).

*5.2.4.5. 2-((1-(4-Fluorophenyl)-1,2-diphenylethyl)sulfanyl)ethanamine (**9e**).* General procedure D with 1-(4-fluorophenyl)-1,2-diphenylethanol (**7e**, 0.800 g, 2.74 mmol) and cysteamine hydrochloride (0.310 g, 2.74 mmol) gave the racemate **9e** (0.085 g, 9%) as a pale yellow gum. ^{1}H NMR (400 MHz): δ ($CDCl_3$): 1.94 (2H, s, NH_2) 2.32 (2H, t, J = 6.4 Hz, CH_2), 2.54 (2H, t, J = 6.4 Hz, CH_2), 3.55–3.61 (2H, m, CH_2), 6.62–6.67 (2H, m), 6.91–7.32 (12H, m). ^{13}C NMR (100 MHz): δ ($CDCl_3$): 31.03, 40.90, 46.85, 60.91, 114.53 (d, J_{CF} = 20.7 Hz), 126.55, 126.97, 127.27, 127.91, 129.00, 130.80 (d, J_{CF} = 7.7 Hz), 131.15, 136.34, 140.48, 144.72, 161.51 (d, J_{CF} = 246.4 Hz). Elemental analysis: Found: C, 71.58; H, 6.11; N, 3.91; S, 8.22 (Required for $C_{22}H_{22}FNS \cdot {}^1/_4 CH_2Cl_2$: C, 71.70; H, 6.08; N, 3.76; S, 8.60). HRMS-ESI (+ve): Calculated for $C_{22}H_{23}FNS$ $(M + H)^+$ 352.1530, found 352.1526. IR: ATR, ν_{max} (cm^{-1}): 3395.4 (NH stretch for primary amine).

*5.2.4.6. 2-((1-(4-Chlorophenyl)-1,2-diphenylethyl)sulfanyl)ethanamine (**9f**).* General procedure D with 1-(4-chlorophenyl)-1,2-diphenylethanol (**7f**, 0.750 g, 2.43 mmol) and cysteamine hydrochloride (0.274 g, 2.43 mmol) gave **9f** as a dark yellow gum (0.150 g, 17%). ^{1}H NMR (400 MHz): δ ($CDCl_3$): 2.20–2.33 (4H, m), 2.55 (2H, t, J = 6.8 Hz, CH_2), 3.53–3.61 (2H, m, CH_2), 6.63–6.67 (2H, m), 7.04–7.27 (12H, m, Ar). ^{13}C NMR (100 MHz): δ ($CDCl_3$): 33.33, 40.69, 46.64, 60.98, 126.61, 127.06, 127.89, 127.96, 128.99, 130.56, 131.14, 132.62, 136.17, 143.32, 144.34. Elemental analysis: Found: C, 66.24; H, 5.72; N, 3.25; (Required for $C_{22}H_{22}ClNS \cdot {}^1/_2 CH_2Cl_2$: 65.85; H, 5.65; N, 3.41). HRMS-ESI (+ve): Calculated for $C_{22}H_{23}(^{35}Cl)NS$ $(M + H)^+$ 368.1230, found 368.1234. Calculated $C_{22}H_{23}(^{37}Cl)N$ S $(M + H)^+$ 370.1205, found 370.1201. IR: ATR, ν_{max} (cm^{-1}): 3545.5 (NH stretch for primary amine).

*5.2.4.7. 2-((1-(4-Methylphenyl)-1,2-diphenylethyl)sulfanyl)ethanamine (**9g**).* General procedure D with 1-(4-methylphenyl)-1,2-diphenylethanol (**7g**, 0.205 g, 0.76 mmol) and cysteamine hydrochloride (0.086 g, 0.76 mmol) gave the racemate **9g** (0.085 g, 18%) as a brown gum. ^{1}H NMR (400 MHz): δ ($CDCl_3$): 2.32 (3H, s, CH_3), 2.42–2.46 (4H, m, CH_2), 3.57 (1H, d, J = 13.7 Hz, CH_2), 3.62 (1H, d, J = 13.7 Hz, CH_2), 6.61–6.65 (2H, m), 7.01–7.30 (12H, m). ^{13}C NMR (100 MHz): δ ($CDCl_3$): 20.98, 31.20, 40.05, 46.71, 61.49, 126.37, 126.69, 127.14, 127.70, 128.45, 129.00, 129.16, 131.18, 136.35, 136.75, 141.90, 144.90. Elemental analysis: Found: C, 75.87; H, 7.42; N, 3.07; S, 8.99 (Required for $C_{23}H_{25}NS \cdot H_2O$: C, 75.57; H, 7.45; N, 3.83; S, 8.77). HRMS-ESI (+ve): Calculated for $C_{23}H_{26}NS$ $(M + H)^+$ 348.1780, found 348.1781. IR: KBr disc, ν_{max} (cm^{-1}): 3434.8 (NH stretch for primary amine).

*5.2.4.8. 2-((1-(4-Hydroxylphenyl)-1,2-diphenylethyl)sulfanyl)ethanamine (**9h**).* General procedure D with 1-(4-hydroxyphenyl)-1,2-diphenylethanol (**7h**, 0.870 g, 3 mmol) and cysteamine hydrochloride (0.340 g, 3 mmol) gave the racemate **9h** (0.100 g, 10%) as a pale yellow gum. ^{1}H NMR (400 MHz): δ (CD_3OD): 2.40–2.43 (2H, m, CH_2), 2.49–2.52 (2H, m, CH_2), 3.61–3.62 (2H, m, CH_2), 6.65–7.32 (14H, m). ^{13}C NMR (100 MHz): δ (CD_3OD): 27.87, 38.94, 46.12, 61.33, 45.86, 61.43, 114.20, 125.95, 126.58, 126.68, 127.46, 128.91, 130.05, 130.99, 135.27, 136.65, 144.81, 156.19. Elemental analysis: Found: C, 65.85; H, 6.35; N, 3.71 (Required for $C_{22}H_{23}NOS$: C, 66.13; H, 5.98; N, 3.39). HRMS-ESI (+ve): Calculated for $C_{22}H_{24}NOS$ $(M + H)^+$ 350.1573, found 350.1576. IR: KBr disc, ν_{max} (cm^{-1}): 3233.3 (OH phenol), 3399.8 (NH stretch for primary amine).

*5.2.4.9. 2-((1-(3,4-Dichlorophenyl)-1,2-diphenylethyl)sulfanyl)ethanamine (**9i**).* General procedure D with 1-(3,4-dichlorophenyl)-1,2-diphenylethanol (**7i**, 1.40 g, 4.0 mmol) and cysteamine hydrochloride (0.454 g, 4.0 mmol) gave the racemate **9i** (0.205 g, 13%) as a pale yellow gum. ^{1}H NMR (400 MHz): δ ($CDCl_3$): 2.21 (2H, s, NH_2) 2.32 (2H, t, J = 6.4 Hz, CH_2), 2.59 (2H, t, J = 6.4 Hz, CH_2), 3.52–3.60 (2H, m), 6.64–6.69 (2H, m), 7.06–7.39 (11H, m). ^{13}C NMR (100 MHz): δ ($CDCl_3$): 33.26, 40.72, 46.53, 60.75, 126.69, 127.31, 128.13, 128.76, 129.63, 130.85, 131.11, 131.92, 135.82, 143.66, 145.27. Elemental analysis: Found: C, 65.31; H, 5.07; N, 3.07; S, 7.53 (Required for $C_{22}H_{21}Cl_2NS \cdot {}^1/_4 H_2O$: C, 64.94; H, 5.33; N, 3.44; S, 7.88). HRMS-ESI (+ve): Calculated for $C_{22}H_{22}(^{35}Cl_2)NS$ $(M + H)^+$ 402.0845, found 402.0846. Calculated $C_{22}H_{22}(^{35}Cl)(^{37}Cl)NS$ $(M + H)^+$ 404.0815, found 404.0811. IR: ATR, ν_{max} (cm^{-1}): 3449.6 (NH stretch for primary amine).

*5.2.4.10. 2-((1-(3-Chlorophenyl)-1-(4-chlorophenyl)-2-phenylethyl) sulfanyl)ethanamine (**9j**).* General procedure D with 1-(3-chlorophenyl)-1-(4-chlorophenyl)-2-phenylethanol (**7m**, 0.519 g, 1.5 mmol) and cysteamine hydrochloride (0.170 g, 1.5 mmol) gave the racemate **9j** (0.057 g, 9%) as a pale yellow gum. ^{1}H NMR (400 MHz): δ ($CDCl_3$): 2.37 (2H, t, J = 6.8 Hz, CH_2), 2.58 (2H, t, J = 6.8 Hz, CH_2), 3.50–3.57 (2H, m, CH_2), 6.62–6.69 (2H, m), 6.92–7.29 (11H, m). ^{13}C NMR (100 MHz): δ ($CDCl_3$): 32.91, 40.62, 46.52, 60.69, 126.81, 127.32, 128.11, 129.06, 129.17, 130.42, 131.10, 132.96, 134.01, 135.69, 142.57, 146.56. Elemental analysis: Found: C, 65.08; H, 5.23; N, 3.02 (Required for $C_{22}H_{21}Cl_2NS \cdot CH_3OH$: C, 64.80; H, 5.49; N, 3.37). HRMS-ESI (+ve): Calculated for $C_{22}H_{22}Cl_2NS$

$(M + H)^+$ 402.0845, found 402.0845. IR: KBr disc, ν_{max} (cm^{-1}): 3434.6 (NH stretch for primary amine).

*5.2.4.11. 2-((1,1-Bis(4-fluorophenyl)-2-phenylethyl)sulfanyl)ethanamine (**9k**).* General procedure D with 1,1-bis(4-fluorophenyl)-2-phenylethanol (**7j**, 1.09 g, 3.5 mmol) and cysteamine hydrochloride (0.398 g, 3.5 mmol) gave **9k** (0.101 g, 8%) as a pale yellow gum. ^{1}H NMR (400 MHz): δ ($CDCl_3$): 1.47 (2H, s, NH_2), 2.27–2.30 (2H, t, J = 6.8 Hz, CH_2), 2.58–2.61 (2H, m, CH_2), 3.54 (2H, s, CH_2), 6.62–6.68 (2H, m), 6.92–7.26 (11H, m). ^{13}C NMR (125 MHz): δ ($CDCl_3$): 33.89, 40.97, 46.94, 60.31, 114.65 (d, J_{CF} = 21.4 Hz), 126.65, 127.34, 130.67 (d, J_{CF} = 8.0 Hz), 131.13, 136.13, 140.45 (d, J_{CF} = 3.1 Hz), 161.55 (d, J_{CF} = 247.4 Hz). Elemental analysis: Found: C, 68.67; H, 5.58; N, 3.60; S, 8.11 (Required for $C_{22}H_{21}F_2NS \cdot ¼CH_2Cl_2$: C, 68.40; H, 5.55; N, 3.58; S, 8.21). HRMS-ESI (+ve): Calculated for $C_{22}H_{22}F_2NS$ $(M + H)^+$ 370.1436, found 370.1432. IR: ATR, ν_{max} (cm^{-1}): 3420.5 (NH stretch for primary amine).

*5.2.4.12. 2-((1,1-Bis(4-chlororophenyl)-2-phenylethyl)sulfanyl)ethanamine (**9l**).* General procedure D with 1,1-bis(4-chlorophenyl)-2-phenylethanol (**7k**, 0.342 g, 1 mmol) and cysteamine hydrochloride (0.113 g, 1 mmol) gave **9l** (0.060 g, 20%) as a white solid. Mpt: 220–221 °C. ^{1}H NMR (400 MHz): δ (CD_3OD): 2.55–2.60 (4H, m, CH_2), 3.65 (2H, s, CH_2), 6.68–6.72 (2H, m), 7.02–7.31 (11H, m). ^{13}C NMR (100 MHz): δ (CD_3OD): 26.90, 38.52, 45.60, 60.87, 126.34, 126.96, 127.79, 130.46, 130.95, 132.82, 135.85, 142.88. Elemental analysis: Found: C, 56.44; H, 4.76; N, 3.23; S, 6.26 (Required for $C_{22}H_{21}Cl_2NS \cdot CH_2Cl_2$: 56.69; H, 4.76; N, 2.87; S, 6.58). HRMS-ESI (+ve): Calculated for $C_{22}H_{22}(^{35}Cl_2)NS$ $(M + H)^+$ 402.0845, found 402.0840. Calculated $C_{22}H_{22}(^{35}Cl)(^{37}Cl)NS$ $(M + H)^+$ 404.0815, found 404.0811. IR: KBr disc, ν_{max} (cm^{-1}): 3412.4 (NH stretch for primary amine).

*5.2.4.13. 2-((1,1-Bis(4-methylphenyl)-2-phenylethyl)sulfanyl)ethanamine (**9m**).* General procedure D with 1,1-bis(4-methylphenyl)-2-phenylethanol (**7l**, 0.302 g, 1 mmol) and cysteamine hydrochloride (0.113 g, 1 mmol) gave **9m** (0.030 g, 8%) as a pale yellow gum. ^{1}H NMR (400 MHz): δ ($CDCl_3$): 2.32 (6H, s, 2 × CH_3), 2.39 (2H, t, J = 5.6 Hz, CH_2), 2.45 (2H, t, J = 5.6 Hz, CH_2), 3.57 (2H, s, CH_2), 3.98 (2H, s, NH_2), 6.62–6.68 (2H, m), 7.02–7.18 (11H, m). ^{13}C NMR (100 MHz): δ (CDCl3): 21.06, 31.33, 40.09, 46.78, 61.35, 126.41, 127.19, 128.57, 128.94, 131.17, 136.56, 136.61, 141.60. Elemental analysis: Found: C, 79.30; H, 7.82; N, 3.89; S, 8.70 (Required for $C_{24}H_{27}NS \cdot {}^1/_5\ CH_3OH$: C, 79.00; H, 7.62; N, 3.81; S, 8.71). HRMS-ESI (+ve): Calculated for $C_{24}H_{28}NS$ $(M + H)^+$ 362.1937, found 362.1934. IR: KBr disc, ν_{max} (cm^{-1}): 3412.4 (NH stretch for primary amine).

*5.2.4.14. 2-((Diphenyl(pyridin-4-yl)methyl)sulfanyl)ethanamine (**18**).* General procedure D with diphenyl(pyridin-4-yl)methanol (0.522 g, 2.75 mmol) and cysteamine hydrochloride (0.310 g, 2.75 mmol) gave after trituration with Et_2O **18** (0.200 g, 18%) as a white solid. Mpt: 178–180 °C. ^{1}H NMR (400 MHz): δ (DMSO-d_6): 2.38 (2H, t, J = 8.4 Hz, CH_2), 2.60 (2H, t, J = 8.0 Hz, CH_2), 7.30–7.42 (12H, m), 8.57–8.61 (2H, m). ^{13}C NMR (125 MHz): δ (DMSO-d_6): 29.09, 37.92, 65.48, 123.84, 127.34, 128.44, 128.88, 142.72, 149.78, 152.52. Elemental analysis: Found: C, 59.78; H, 5.32; N, 6.94; S, 7.35 (Required for $C_{20}H_{20}N_2S \cdot CH_2Cl_2$: C, 59.83; H, 5.32; N, 6.57; S, 7.51).

HRMS-ESI (+ve): Calculated for $C_{20}H_{21}N_2S$ $(M + H)^+$ 321.1420, found 321.1416.

*5.2.4.15. 2-((2-Aminoethyl)sulfanyl)-1,2,2-triphenylethanone (**19**).* General procedure D with 2-hydroxy-1,2,2-triphenylethanone (**13**, 0.158 g, 0.75 mmol) and cysteamine hydrochloride (0.085 g, 0.75 mmol) gave a yellow gum **19** (0.100 g, 41%). ^{1}H NMR (400 MHz): δ ($CDCl_3$): 2.41 (2H, t, J = 6.0 Hz, CH_2), 2.81 (2H, t, J = 6.0 Hz, CH_2), 6.21 (2H, s, NH_2), 7.14–7.49 (13H, m), 7.64–7.66 (2H, m). ^{13}C NMR (100 MHz): δ (CDCl3): 25.46, 39.00, 48.96, 127.26, 127.42, 127.94, 128.67, 129.38, 130.43, 130.95, 132.65, 135.64, 138.76, 142.05, 198.65. Elemental analysis: Found: C, 76.80; H, 6.08; N, 4.32; S, 8.89 (Required for $C_{22}H_{21}NOS$: C, 76.04; H, 6.09; N, 4.03; S, 9.23). HRMS-ESI (+ve): Calculated for $C_{22}H_{22}NOS$ $(M + H)^+$ 348.1417, found 348.1408. IR: KBr disc, ν_{max} (cm^{-1}): 1684.8 (C=O stretch for ketone), 3434.6 (NH stretch for primary amine).

*5.2.4.16. 2-(Tritylthio)ethanamine (**17**).* Compound **17** was prepared by an adaption of the procedure reported by Maltese et al. [47]. A solution of trityl alcohol (1.95 g, 7.5 mmol) and cysteamine hydrochloride (0.937 g, 8.25 mmol) in trifluoroacetic acid (7.5 mL) was stirred for 3 h at room temperature. The volatiles were evaporated under reduced pressure, and the crude residue basified (*circa.* pH 10) with saturated aqueous Na_2CO_3 solution. The aqueous mixture was extracted with CH_2Cl_2 (3 × 10 mL), the organic layer was dried ($MgSO_4$) and evaporated under reduced pressure. The residue was then purified by flash column chromatography [MeOH:CH_2Cl_2 (10:90)] to give compound **17** (1.94 g, 81%) as a white powder. Mpt: 87–90 °C (lit. 90–93 °C from petroleum ether) [48]. ^{1}H NMR (500 MHz): δ (MeOD): 2.32–2.36 (m, 2H, CH_2), 2.41–2.45 (m, 2H, CH_2), 7.19–7.24 (m, 3H), 7.25–7.31 (m, 6H), 7.39–7.41 (m, 6H). ^{13}C NMR (125 MHz): δ (MeOD): 6.11, 41.56, 67.77, 127.79, 128.89, 130.78, 146.34. HRMS-ESI (+ve): Calculated for $C_{21}H_{22}NS$ $(M + H)^+$: 320.1467, found 320.1466. Elemental analysis: Found: C, 78.96; H, 6.63; N, 4.20 (Required for $C_{21}H_{21}NS$: C, 78.95; H, 6.63; N, 4.38).

5.3. Biological materials and methods

HCT116 (ATCC CCL-247) cells were cultured in DMEM (Invitrogen, Paisley, UK), supplemented with 10% foetal bovine serum (PAA, Pasching, Austria). K562 (ATC CCCL-243) and NCI-H1299 (CRL-5803) cells were cultured in RPMI (Invitrogen, Paisley, UK), supplemented with 10% foetal bovine serum (PAA, Pasching, Austria). BxPC-3 (ATCC CRL-1687) cells were cultured in RPMI (Invitrogen, Paisley, UK), supplemented with 1% nonessential amino acids (Invitrogen, Paisley, UK), 1% sodium pyruvate (Invitrogen, Paisley, UK), 1% glutamine (Invitrogen, Paisley, UK), and 10% foetal bovine serum (PAA, Pasching, Austria). KB-3-1 (DSMZ ACC 158) cells were cultured in DMEM (Invitrogen, Paisley, UK), supplemented with 1% sodium pyruvate (Invitrogen, Paisley, UK), 1% glutamine (Invitrogen, Paisley, UK), and 10% foetal bovine serum (PAA, Pasching, Austria). KB-V1 (DSMZ ACC 149) was cultured in DMEM (Invitrogen, Paisley, UK), supplemented with 1% glutamine (Invitrogen, Paisley, UK) and 15% foetal bovine serum (PAA, Pasching, Austria). To maintain mdr1 mRNA overexpression, media also contained 600 ng/mL of vinblastine. All cells were maintained at 37 °C, 95% humidity, and 5% carbon dioxide in a humidified incubator. They were used for experiments for 6–8 weeks before they were replaced with fresh stocks, which are stored in liquid nitrogen.

5.3.1. Inhibition of the basal Eg5 ATPase activity (IC_{50})

Inhibitor analogues were measured as recently described using the coupled pyruvate kinase/lactate dehydrogenase assay [16]. All compounds were measured once to determine their initial IC_{50} values and separate compounds that inhibit basal Eg5 activity from those that do not. If necessary, the inhibitor concentrations were adjusted and the inhibition of the basal Eg5 activity of the active compounds was then measured in triplicate at 25 °C using a TECAN Sunrise photometer (Maennedorf, Switzerland). The data were analyzed using Excel and Kaleidagraph 3.0 (Synergy Software, Reading, USA).

5.3.2. Cell proliferation assays

Compounds that inhibited of Eg5 activity *in vitro* with $IC_{50} < 180$ nM were tested to determine their growth inhibition effect (GI_{50}) in the human leukaemic cell line K562. Six selected inhibitors (**4**, **8a**, **8f**, **8g**, **9f** and **9g**) were tested in three additional tumour cell lines of various tissue origins (BxPC-3, HCT116 and NCI-H1299). Experimental procedures were as described in reference [49]. Briefly, cells were seeded in triplicate in 96-well assay plates at 1250 cells (BxPC-3, HCT116), 2500 cells (NCI-H1299), or 5000 cells (K562) per well in 100 μL of the respective growth medium. Medium blanks (without any cells) and cell blanks (without any inhibitors) for every cell line were also prepared. On the next day, inhibitors were added with a starting concentration of 100 μM in a 3-fold serial dilution series. After 72 h post inhibitor addition, 10% Alamar Blue (Invitrogen, Paisley, UK) was added and depending on the cell line, 2–12 h later the absorbance was measured at 570 and 600 nm. All values were corrected for the absorbance of the medium blank and the corrected cell blanks were set to 100%. Calculations for determining the relative proliferation were performed using equations described in the manufacturer's manual. Finally, the GI_{50} values were determined using a sigmoidal dose–response fitting (variable slope) with GraphPad Prism 5.01 for Windows (GraphPad Software, San Diego, USA).

5.3.3. MDR cell assays

Experimental procedures were as described in Ref. [49]. Briefly, cells were seeded in triplicates in 96-well assay plates at 2000 cells (KB-3-1 and KB-V1) per well in 100 μL of the respective growth medium. The setup and measurements of the assay are identical to the proliferation assay described before. The MDR ratio was calculated by dividing the GI_{50} value for a particular drug in the mdr1-overexpressing KB-V1 cells by the GI_{50} value obtained in the parental KB-3-1 cells. Thus, if an inhibitor is a substrate for mdr1, KB-V1 cells will be more resistant to its antiproliferative effects than KB-3-1 cells, resulting in an MDR ratio greater than 1.

5.3.4. Solubility measurements

To determine turbidimetric solubility, compounds **4**, **8a**, **8g**, **9a** and **9g** were measured at 1 μM, 3 μM, 10 μM, 30 μM and 100 μM at a final DMSO concentration of 1% in 10 mM phosphate buffered saline at pH 7.4. Pyrene and Nicardipine were used as controls. The temperature was 37 °C with an incubation time of 2 h and the turbidimetry was measured at a wavelength of 620 nm. The number of replicates was $n = 7$.

Acknowledgements

We thank Cancer Research UK and the University of Strathclyde for financial support. We thank Kristal Kaan and Sandeep Talapatra for providing us with purified human Eg5 for ATPase assays.

Appendix A. Supplementary material

Supplementary data associated with this article can be found, in the online version, at http://dx.doi.org/10.1016/j.ejmech.2012.05.034.

References

[1] M.A. Jordan, L. Wilson, Microtubules as a target for anticancer drugs, Nature Reviews Cancer 4 (2004) 253–265.
[2] K.E. Sawin, K. LeGuellec, M. Philippe, T.J. Mitchison, Mitotic spindle organization by a plus-end-directed microtubule motor, Nature 359 (1992) 540–543.
[3] A. Blangy, H.A. Lane, P. d'Hérin, M. Harper, M. Kress, E.A. Niggt, Phosphorylation by p34cdc2 regulates spindle association of human Eg5, a kinesin-related motor essential for bipolar spindle formation in vivo, Cell 83 (1995) 1159–1169.
[4] M. Shimizu, H. Ishii, N. Ogo, Y. Unno, K. Matsuno, J.-i. Sawada, Y. Akiyama, A. Asai, S-trityl-L-cysteine derivative induces caspase-independent cell death in K562 human chronic myeloid leukemia cell line, Cancer Letters 298 (2010) 99–106.
[5] F. Kozielski, D.A. Skoufias, R.L. Indorato, Y. Saoudi, P.R. Jungblut, H.K. Hustoft, M. Strozynski, B. Thiede, Proteome analysis of apoptosis signaling by S-trityl-L-cysteine, a potent reversible inhibitor of human mitotic kinesin Eg5, Proteomics 8 (2008) 289–300.
[6] D. Huszar, M.E. Theoclitou, J. Skolnik, R. Herbst, Kinesin motor proteins as targets for cancer therapy, Cancer Metastasis Reviews 28 (2009) 197–208.
[7] L. Lad, L. Luo, J.D. Carson, K.W. Wood, J.J. Hartman, R.A. Copeland, R. Sakowicz, Mechanism of inhibition of human KSP by ispinesib, Biochemistry 47 (2008) 3576–3585.
[8] C.W. Lee, K. Belanger, S.C. Rao, T.M. Petrella, R.G. Tozer, L. Wood, K.J. Savage, E.A. Eisenhauer, T.W. Synold, N. Wainman, L. Seymour, A phase II study of ispinesib (SB-715992) in patients with metastatic or recurrent malignant melanoma: a National Cancer Institute of Canada Clinical Trials Group trial, Investigational New Drugs 26 (2008) 249–255.
[9] T. Beer, B. Goldman, T. Synold, C. Ryan, L. Vasist, P. Van Veldhuizen Jr., S. Dakhil, P. Lara Jr., A. Drelichman, M. Hussain, E.D. Crawford, Southwest Oncology Group Phase II Study of ispinesib in androgen-independent prostate cancer previously treated with taxanes, Clinical Genitourinary Cancer 6 (2008) 103–109.
[10] H. Burris, S. Jones, D. Williams, S. Kathman, J. Hodge, L. Pandite, P. Ho, S. Boerner, P. LoRusso, A phase I study of ispinesib, a kinesin spindle protein inhibitor, administered weekly for three consecutive weeks of a 28-day cycle in patients with solid tumors, Investigational New Drugs 29 (2011) 467–472.
[11] S. DeBonis, D.A. Skoufias, L. Lebeau, R. Lopez, G. Robin, R.L. Margolis, R.H. Wade, F. Kozielski, In vitro screening for inhibitors of the human mitotic kinesin Eg5 with antimitotic and antitumor activities, Molecular Cancer Therapeutics 3 (2004) 1079–1090.
[12] S. DeBonis, D.A. Skoufias, R.-L. Indorato, F. Liger, B. Marquet, C. Laggner, B. Joseph, F. Kozielski, Structure-activity relationship of *S*-trityl-L-cysteine analogues as inhibitors of the human mitotic kinesin Eg5, Journal of Medicinal Chemistry 51 (2008) 1115–1125.
[13] H.Y.K. Kaan, V. Ulaganathan, D.D. Hackney, F. Kozielski, An allosteric transition trapped in an intermediate state of a new kinesin–inhibitor complex, Biochemical Journal 425 (2009) 55–60.
[14] E.D. Kim, R.S. Buckley, S. Learman, J. Richard, C. Parke, D.K. Worthylake, E.J. Wojcik, R.A. Walker, S. Kim, Allosteric drug discrimination is coupled to mechanochemical changes in the kinesin-5 motor core, Journal of Biological Chemistry 285 (2010) 18650–18661.
[15] N. Ogo, S. Oishi, K. Matsuno, J.-i. Sawada, N. Fujii, A. Asai, Synthesis and biological evaluation of L-cysteine derivatives as mitotic kinesin Eg5 inhibitors, Bioorganic & Medicinal Chemistry Letters 17 (2007) 3921–3924.
[16] H.Y.K. Kaan, J. Weiss, D. Menger, V. Ulaganathan, K. Tkocz, C. Laggner, F. Popowycz, B.t. Joseph, F. Kozielski, Structure–activity relationship and multidrug resistance study of new *S*-trityl-L-Cysteine derivatives as inhibitors of Eg5, Journal of Medicinal Chemistry 54 (2011) 1576–1586.
[17] D. Rodriguez, C. Ramesh, L.H. Henson, L. Wilmeth, B.K. Bryant, S. Kadavakollu, R. Hirsch, J. Montoya, P.R. Howell, J.M. George, D. Alexander, D.L. Johnson, J.B. Arterburn, C.B. Shuster, Synthesis and characterization of tritylthioethanamine derivatives with potent KSP inhibitory activity, Bioorganic & Medicinal Chemistry 19 (2011) 5446–5453.
[18] M. Hatano, S. Suzuki, K. Ishihara, Highly efficient alkylation to ketones and aldimines with Grignard reagents catalyzed by zinc(II) chloride, Journal of the American Chemical Society 128 (2006) 9998–9999.
[19] R.P. Boivin, V. Luu-The, R. Lachance, F. Labrie, D. Poirier, Structure-activity relationships of 17α derivatives of estradiol as inhibitors of steroid sulfatase, Journal of Medicinal Chemistry 43 (2000) 4465–4478.
[20] G.S. Silverman, P.E. Rakita, Handbook of Grignard Reagents, Marcel Dekker, New York, 1996.
[21] J. Srinivasan, T.E. Cheatham, P. Cieplak, P.A. Kollman, D.A. Case, Continuum solvent studies of the stability of DNA, RNA, and phosphoramidate-DNA helices, Journal of the American Chemical Society 120 (1998) 9401–9409.
[22] Z. Maliga, T.M. Kapoor, T.J. Mitchison, Evidence that monastrol is an allosteric inhibitor of the mitotic kinesin Eg5, Chemistry & Biology 9 (2002) 989–996.
[23] S. DeBonis, J.-P. Simorre, I. Crevel, L. Lebeau, D.A. Skoufias, A. Blangy, C. Ebel, P. Gans, R. Cross, D.D. Hackney, R.H. Wade, F. Kozielski, Interaction of the mitotic inhibitor monastrol with human kinesin Eg5, Biochemistry 42 (2003) 338–349.
[24] G. Huchet, M.R. Euerby, S.P. Mackay, R.D. Waigh, The role of water in drug–receptor interactions, Journal of Enzyme Inhibition and Medicinal Chemistry 21 (2006) 271–276.
[25] M. Kontoyianni, L.M. McClellan, G.S. Sokol, Evaluation of docking performance: comparative data on docking algorithms, Journal of Medicinal Chemistry 47 (2003) 558–565.
[26] C.D. Cox, M.J. Breslin, B.J. Mariano, P.J. Coleman, C.A. Buser, E.S. Walsh, K. Hamilton, H.E. Huber, N.E. Kohl, M. Torrent, Y. Yan, L.C. Kuo, G.D. Hartman, Kinesin spindle protein (KSP) inhibitors. Part 1: the discovery of 3,5-diaryl-4,5-dihydropyrazoles as potent and selective inhibitors of the mitotic kinesin KSP, Bioorganic & Medicinal Chemistry Letters 15 (2005) 2041–2045.
[27] K. Schiemann, D. Finsinger, F. Zenke, C. Amendt, T. Knöchel, D. Bruge, H.-P. Buchstaller, U. Emde, W. Stähle, S. Anzali, The discovery and optimization of

hexahydro-2H-pyrano[3,2-c]quinolines (HHPQs) as potent and selective inhibitors of the mitotic kinesin-5, Bioorganic & Medicinal Chemistry Letters 20 (2010) 1491–1495.
[28] M.J. Waring, Lipophilicity in drug discovery, Expert Opinion on Drug Discovery 5 (2010) 235–248.
[29] M.M. Gottesman, T. Fojo, S.E. Bates, Multidrug resistance in cancer: role of ATP-dependent transporters, Nature Reviews Cancer 2 (2002) 48–58.
[30] S. Ding, K. Nishizawa, T. Kobayashi, S. Oishi, J. Lv, N. Fujii, O. Ogawa, H. Nishiyama, A potent chemotherapeutic strategy for bladder cancer: (*S*)-methoxy-trityl-L-cystein, a novel Eg5 inhibitor, The Journal of Urology 184 (2010) 1175–1181.
[31] C. Wiltshire, B.L. Singh, J. Stockley, J. Fleming, B. Doyle, R. Barnetson, C.N. Robson, F. Kozielski, H.Y. Leung, Docetaxel-resistant prostate cancer cells remain sensitive to *S*-trityl-L-cysteine-mediated Eg5 inhibition, Molecular Cancer Therapeutics 9 (2010) 1730–1739.
[32] L. Yang, C.-h. Tan, M.-J. Hsieh, J. Wang, Y. Duan, P. Cieplak, J. Caldwell, P.A. Kollman, R. Luo, New-generation amber united-atom force field, The Journal of Physical Chemistry B 110 (2006) 13166–13176.
[33] D.A. Case, T.A. Darden, T.E. Cheatham III, C.L. Simmerling, J. Wang, R.E. Duke, R. Luo, K.M. Merz, D.A. Pearlman, M. Crowley, R.C. Walker, W. Zhang, B. Wang, S. Hayik, A. Roitberg, G. Seabra, K.F. Wong, F. Paesani, X. Wu, S. Brozell, V. Tsui, H. Gohlke, L.J. Yang, C.H. Tan, J. Mongan, V. Hornak, G. Cui, P. Beroza, D.H. Mathews, C. Schafmeister, W.S. Ross, P.A. Kollman, AMBER 9, University of California, San Francisco, 2006.
[34] U.C. Singh, P.A. Kollman, An approach to computing electrostatic charges for molecules, Journal of Computational Chemistry 5 (1984) 129–145.
[35] F. Fogolari, A. Brigo, H. Molinari, Protocol for MM/PBSA molecular dynamics simulations of proteins, Biophysical Journal 85 (2003) 159–166.
[36] A.K. Ghose, V.N. Viswanadhan, J.J. Wendoloski, Prediction of hydrophobic (lipophilic) properties of small organic molecules using fragmental methods: an analysis of ALOGP and CLOGP Methods, The Journal of Physical Chemistry A 102 (1998) 3762–3772.
[37] I.V. Tetko, V.Y. Tanchuk, T.N. Kasheva, A.E.P. Villa, Estimation of aqueous solubility of chemical compounds using E-state indices, Journal of Chemical Information and Computer Sciences 41 (2001) 1488–1493.
[38] W.C. Still, M. Kahn, A. Mitra, Rapid chromatographic technique for preparative separations with moderate resolution, The Journal of Organic Chemistry 43 (1978) 2923–2925.
[39] W. Schöniger, Eine mikroanalytische Schnellbestimmung von Halogen in organischen Substanzen, Microchimica Acta 43 (1955) 123–129.
[40] J.F. Eastham, D.Y. Cannon, Ortho-substitution of benzyl-type Grignard reagents by cyanogen and thiocyanogen, The Journal of Organic Chemistry 25 (1960) 1504–1506.
[41] C.F. Koelsch, Syntheses with triarylvinylmagnesium bromides. Triarylacrylic acids and the indones derived from them, Journal of the American Chemical Society 54 (1932) 2487–2493.
[42] L.L. Alexander, R.C. Fuson, Reversibility of the Friedel-Crafts reaction. Hydrogenation, Journal of the American Chemical Society 58 (1936) 1745–1747.
[43] E.A. Adegoke, T.A. Emokpae, H. Ephraim-Bassey, C.A. Oyelola, Synthesis of 3-benzoyl-3,4-dihydro-2H- and 3,4-dihydro-2,2-disubstituted-benzopyrans via alkynyl Grignard reagents, Journal of Heterocyclic Chemistry 24 (1987) 1705–1708.
[44] C.L. Stevens, J.J. DeYoung, Epoxy ethers. VI. A triphenyl substituted epoxy ether, Journal of the American Chemical Society 76 (1954) 718–720.
[45] A.P. Orechov, R. Grinberg, Syntheses in the indene series. 111. Synthesis of phenylbenzylindene, Journal of the Chemical Society, Abstracts 112 (1917) i450–i451.
[46] W. Tadros, K. Farahat, J.M. Robson, 100. Synthetic estrogens related to triphenylethylene, Part I, Journal of the Chemical Society (Resumed), (1949) 439–441.
[47] M. Maltese, Reductive demercuration in deprotection of trityl thioethers, trityl amines, and trityl ethers, The Journal of Organic Chemistry 66 (2001) 7615–7625.
[48] F.I. Carroll, H.M. Dickson, M.E. Wall, Organic sulfur compounds. III. Synthesis of 2-(substituted alkylamino)ethanethiols, The Journal of Organic Chemistry 30 (1965) 33–38.
[49] H.Y.K. Kaan, V. Ulaganathan, O. Rath, H. Prokopcova, D. Dallinger, C.O. Kappe, F. Kozielski, Structural basis for inhibition of Eg5 by dihydropyrimidines: stereoselectivity of antimitotic inhibitors enastron, dimethylenastron and fluorastrol, Journal of Medicinal Chemistry 53 (2010) 5676–5683.